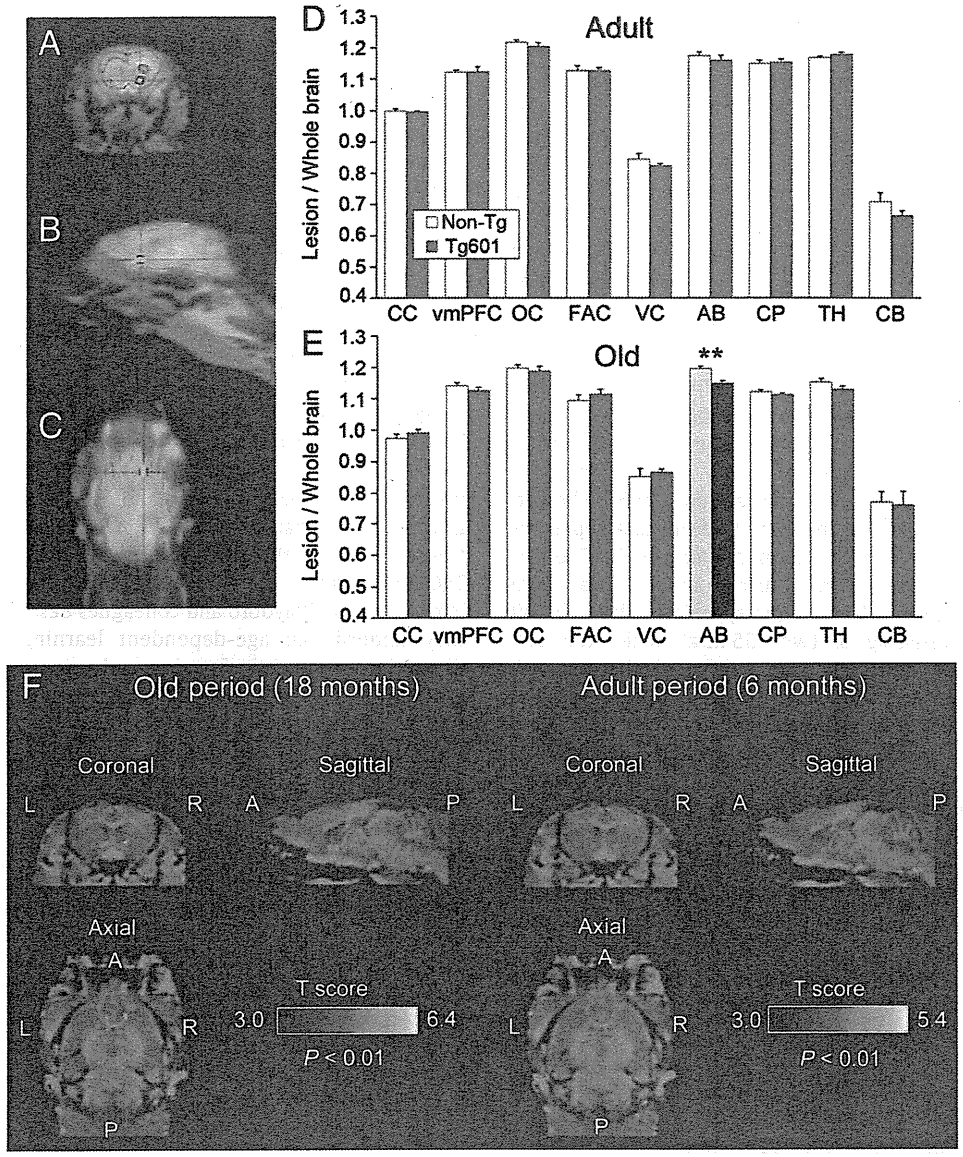

Fig. 7. Glucose hypometabolism in the nucleus accumbens in the old Tg601 mice. A–C, Volumetric regions of interest (ROIs) were manually placed on several brain regions according to the fused 2-[^{18}F]fluoro-2-deoxy-D-glucose ([^{18}F]FDG) PET/MR T1-weighted images of control mouse. Representative regions are shown. Other ROIs are shown in Supplemental Fig. 6. D, E, FDG uptake ratio in the accumbens in old Tg601 mice (n = 5) was significantly lower than that of non-Tg mice (n = 5) (**P = 0.004; Student's t-test), while no significant difference was seen between adult Tg601 mice (n = 4) and non-Tg mice (n = 6). F, The regions with statistically significant decreases in retention of [^{18}F]FDG in Tg601 mice compared with those in non-Tg mice are highlighted by SPM analysis. Old Tg601 mice exhibited significantly decreased [^{18}F]FDG retention exclusively in the nucleus accumbens. CC, cerebral cortex; vmPFC, ventral medial prefrontal cortex; OC, orbital cortex; VC, visual cortex; FAC, frontal association cortex; AB, nucleus accumbens; CP, caudate putamen; TH, thalamus; CB, cerebellum.

2003). The Acb is involved in eliciting appropriate emotional behavior as well as in processes such as motivation, reward, and locomotion (Cardinal et al., 2002; Kalivas and Nakamura, 1999). The AMPA receptor blockade in the Acb shell was reported to induce anxiolytic-like effects, such as an increase in open arm avoidance in the EPM (da Cunha et al., 2008). NMDA and non-NMDA-glutamatergic blockade in the Acb at higher doses had a comparable effect (Martinez et al., 2002). Neuroanatomically, glutamatergic projection emerging from the medial PFC, basolateral amygdala, and hippocampal formation, important regions for emotional processing and regulation, converge on spiny neurons of the Acb (Pennartz et al., 1994).

In the striatum of old Tg601 mice, AT8-positive tau was decreased compared with that in other regions, while PHF-1 site phosphorylated tau levels remained equal. Immunohistochemical results revealed that this difference was not observed in young Tg601. It is likely that PHF-1 site phosphorylated tau would be more closely related to synapse loss than AT8-positive or AT180-positive tau in the Acb of Tg601 mice. Ser^{396}-phosphorylated tau construct has a weakened ability to bind MTs and promote MT assembly and MT structure stabilization (Bramblett et al., 1993). It has been suggested that phosphorylation of tau on Ser^{396} causes a conformational change in tau that accelerates tau aggregation in AD brain (Alonso et al., 2006). Fluorescence resonance energy transfer (FRST) analysis demonstrated that pseudophosphorylation at the PHF-1 epitope moves the C-terminal domain away from the repeat domain and this is accompanied by a strong increase in the reaction with conformation-dependent antibody MC1 (Jeganathan et al., 2008). Thus, hyperphosphorylated tau at the PHF-1 epitope might detach from MTs and disturb the synaptic function in the Acb of Tg601. The developmental regulation of tau phosphorylation at various sites was studied in rats during development (Yu et al., 2009). Tau phosphorylation at various sites had different topographic distributions. It was suggested that several tau kinases might regulate tau phosphorylation. In Tg601 mouse brain, several tau kinases might regulate tau phosphorylation in various regions.

In the PFC of Tg601 mice, progressive morphological changes including axonal swelling and spheroids, histopathological correlates of disrupted axonal transport, were observed. The rat PFC consists of cytoarchitecturally and functionally distinct areas located over the medial, orbital, and insular surfaces of the rostral cerebral hemispheres. The medial PFC and orbitofrontal cortex are involved in both cognitive and emotion functions whereas the insular cortex is primarily a viscerosensory region (Schoenbaum et al., 2003; Uylings et al., 2003). Wheat germ agglutinin conjugated with horseradish peroxidase (WGA-HRP) tracer injections into the Acb in the rat predominantly labeled populations of neurons located in layers II, V, and VI of the medial PFC and in layer V of the orbital cortex (Gabbott et al., 2005). Since, in Tg601 mice, axonal dilatations were mainly observed in layers V and VI but not in layer I or III in the medial PFC and the orbital cortex, we postulate that the disruption of axonal transport of the PFC–Acb pathway may have occurred in Tg601 mice.

Tau multimer (140 kDa) was present in the soluble fraction of Tg601 brain tissue and increased with aging, although Tg601 showed neither insoluble tau nor NFTs. We speculate that this may represent tau dimer consisting of two "55 kDa" tau monomers. In rTg4510 and JNPL3 mice, two forms of multimers (140 kDa and 170 kDa) were described (Berger et al., 2007). The authors speculated that tau 140 represented dimers consisting of two "55 kDa" while tau 170 contained two "64 kDa" and they also suggested the tau 140 multimers were the earliest pathological species. "64 kDa" tau has been considered to represent insoluble tau and NFTs in rTg4510 and JNPL3 mice (Berger et al., 2007; Sahara et al., 2002). Since, in Tg601 mice, NFTs did not appear at 20 months, "170 kDa" tau multimer might not emerge. Generally, tau Tg mice overexpressing wild-type tau did not form NFTs unless the mice reached a very old age (Andorfer et al., 2003; Brion et al., 1999; Gotz et al., 1995; Ishihara et al., 1999, 2001; Kimura et al., 2007; Probst et al., 2000; Spittaels et al., 1999). Tg601 demonstrated, for the first time, the presence of soluble tau multimer among tau Tg mice overexpressing wild-type tau. In vitro heparin-induced assembly of recombinant tau revealed that an increase of tau multimer was observed prior to the detection of increased thioflavin T fluorescence signals (Sahara et al., 2007). Increasing evidence suggests that NFT per se might be dissociated with neuronal dysfunction and the other species that occur during NFT formation (Santacruz et al., 2005; Spires et al., 2006) might cause synaptic dysfunction (Polydoro et al., 2009). Soluble tau multimer may be necessary to reach filamentous structure and may cause behavioral dysfunction in tau Tg mice.

Tg601 mice may be a unique model for FTLD because decreased anxiety behavior is reminiscent of a characteristic symptom, disinhibition, which frequently occurs in patients with FTLD. Moreover, observation of decreased Y-maze spontaneous alternation is potentially consistent with the idea that the animals have impaired working memory and resection of prefrontal cortex of the mice leads to impaired spontaneous alternation in Y-maze test (Mogensen and Divac, 1993). Since, immunohistochemically, Tg601 mice displayed axonal dilatations in the prefrontal cortex, we postulate that Tg601 could be a model of FTLD. Recently, the Acb has been described as being involved in the disease of FTLD. Voxel-based morphometry of MRI was performed for patients with a clinical diagnosis of FTLD (Zamboni et al., 2008) and this analysis demonstrated that the severity of disinhibition was correlated with atrophy in the right Acb. The Acb plays a key role in limbic circuits that are responsible for motivated, goal-directed behaviors (Morgane et al., 2005). These findings support the notion that the PFC–Acb projection is involved in FTLD, which is consistent with our result for Tg601 mice.

Patients with FTLD have shown memory impairment, although a predominant feature is change in personal and social behaviors often associated with disinhibition (Lee et al., 2001). The Tg601 mice present with impairment in spatial learning and memory without decreased glucose metabolism in the entorhinal cortex, hippocampus, and the piriform cortex. This result could be due to the synapse loss in the Acb as the Acb is involved in consolidation of information necessary for spatial learning (Sargolini et al., 2003). THY-tau 22 mouse model, which expresses tau mutated at sites G272V and P301S, also showed both decreased anxiety in the EPM and impaired learning in the MWM (Schindowski et al., 2006). The authors described decreased hippocampal synaptic transmission but not the function of amygdala or prefrontal cortex. V337M tau Tgs also demonstrated increased time spent in open arms in the EPM, although this was not accompanied by impaired spatial learning in the MWT (Tanemura et al., 2002). They also showed decreased hippocampal activity.

The phenotype of Tg601 mice was different from that of WTau-Tg, which we previously described (Kimura et al., 2007), although wild-type human tau (2N4R) was expressed under the CAMKIIαpromoter in both of these mice. WTau-Tg mice showed hyperphosphorylated tau in parahippocampal cortex and impaired place learning while Tg601 mice displayed decreased anxiety. In Tg601 mice, the total protein level of the transgenic tau in the cortex was almost the same as that of the striatum, while Wtau-Tg showed higher expression of transgenic tau in the striatum than in the cortex. In the striatum of Tg601 mice, transgenic tau may be more hyperphosphorylated than in Wtau-Tg mice. Polydoro and colleagues described that tau pathology may underlie an age-dependent learning impairment through disruption of synaptic function and our results support this idea. Furthermore, we also demonstrated that hyperphosphorylated tau at PHF-1 epitope and oligomeric soluble tau, not insoluble filamentous tau, may cause synapse loss.

Conclusion

We generated a four-repeat (4R) tauopathy model mouse that exhibited synapse loss in the Acb and axonopathy in the PFC. We postulate that hyperphosphorylated tau at PHF-1 epitope in the striatum may cause synapse loss in the Acb. In the brain of sporadic 4R tauopathies including PSP, CBD, and AGD, phosphorylated tau pathologies were observed in the subcortical nuclei. Altered distribution pattern of soluble hyperphosphorylated tau may contribute to region-specific neurodegeneration, which occurs in various tauopathies.

Supplementary materials related to this article can be found online at doi:10.1016/j.nbd.2011.02.002.

Acknowledgment

We are grateful to Mrs. Miyuki Kunichika for excellent technical assistance regarding silver staining.

References

Alonso, A.C., Zaidi, T., Grundke-Iqbal, I., Iqbal, K., 1994. Role of abnormally phosphorylated tau in the breakdown of microtubules in Alzheimer disease. Proc. Natl. Acad. Sci. USA 91, 5562–5566.

Alonso, A.C., Li, B., Grundke-Iqbal, I., Iqbal, K., 2006. Polymerization of hyperphosphorylated tau into filaments eliminates its inhibitory activity. Proc. Natl. Acad. Sci. USA 103, 8864–8869.

Andorfer, C., Kress, Y., Espinoza, M., de Silva, R., Tucker, K.L., Barde, Y.A., Duff, K., Davies, P., 2003. Hyperphosphorylation and aggregation of tau in mice expressing normal human tau isoforms. J. Neurochem. 386, 582–590.

Arendash, G.W., Lewis, J., Leighty, R.E., McGowan, E., Cracchiolo, J.R., Hutton, M., Garcia, M.F., 2004. Multi-metric behavioral comparison of APPsw and P301L models for Alzheimer's disease: linkage of poorer cognitive performance to tau pathology in forebrain. Brain Res. 1012, 29–41.

Augustinack, J.C., Schneider, A., Mandelkow, E.M., Hyman, B.T., 2002. Specific tau phosphorylation sites correlate with severity of neuronal cytopathology in Alzheimer's disease. Acta Neuropathol. 103, 26–35.

Ballatore, C., Lee, V.M., Trojanowski, J.Q., 2007. Tau-mediated neurodegeneration in Alzheimer's disease and related disorders. Nat. Rev. Neurosci. 8, 663–672.

Berger, Z., Roder, H., Hanna, H., Carlson, A., Rangachari, V., Yue, M., Wezolek, Z., Ashe, K., Knight, J., Dickson, D., Andorfer, C., Rosenberry, T.L., Lewis, J., Hutton, M., Janus, C., 2007. Accumulation of pathological tau species and memory loss in a conditional model of tauopathy. J. Neurosci. 27, 3650–3662.

Biernat, J., Gustke, N., Drewes, G., Mandelkow, E.M., Mandelkow, E., 1993. Phosphorylation of Ser262 strongly reduces binding of tau to microtubules: distinction between PHF-like immunoreactivity and microtubule binding. Neuron 11, 153–163.
Boeve, B.F., Hutton, M., 2008. Refining frontotemporal dementia with parkinsonism linked to chromosome 17: introducing FTDP-17 (MAPT) and FTDP-17 (PGRN). Arch. Neurol. 65, 460–464.
Bramblett, G.T., Goedert, M., Jakes, R., Merrick, S.E., Trojanowski, J.Q., Lee, V.M., 1993. Abnormal tau phosphorylation at Ser396 in Alzheimer's disease recapitulates development and contributes to reduced microtubule binding. Neuron 10, 1089–1099.
Brion, J.P., Smith, C., Couck, A.M., Gallo, J.M., Anderton, B.H., 1993. Developmental changes in tau phosphorylation: fetal tau is transiently phosphorylated in a manner similar to paired helical filament-tau characteristic of Alzheimer's disease. J. Neurochem. 61, 2071–2080.
Brion, J.P., Tremp, G., Octave, J.N., 1999. Transgenic expression of the shortest human tau affects its compartmentalization and its phosphorylation as in the pretangle stage of Alzheimer's disease. Am. J. Pathol. 154, 255–270.
Cairns, N.J., Bigio, E.H., Mackenzie, I.R., Neumann, M., Lee, V.M., Hatanpaa, K.J., White III, C.L., Schneider, J.A., Grinberg, L.T., Halliday, G., Duyckaerts, C., Lowe, J.S., Holm, I.E., Tolnay, M., Okamoto, K., Yokoo, H., Murayama, S., Woulfe, J., Munoz, D.G., Dickson, D.W., Ince, P.G., Trojanowski, J.Q., Mann, D.M., Consortium for Frontotemporal Lobar Degeneration, 2007. Neuropathologic diagnostic and nosologic criteria for frontotemporal lobar degeneration: consensus of the Consortium for Frontotemporal Lobar Degeneration. Acta Neuropathol. 114, 5–22.
Cardinal, R.N., Parkinson, J.A., Hall, J., Everitt, B.J., 2002. Emotion and motivation: the role of the amygdala, ventral striatum, and prefrontal cortex. Neurosci. Biobehav. Rev. 26, 321–352.
da Cunha, I.C., Lopes, A.P., Steffens, S.M., Ferraz, A., Vargas, J.C., de Lima, T.C., Marino Neto, J., Paschoalini, M.A., Faria, M.S., 2008. The microinjection of AMPA receptor antagonist into the accumbens shell, but not into the accumbens core, induces anxiolysis in an animal model of anxiety. Behav. Brain Res. 188, 91–99.
Dawson, H.N., Cantillana, V., Chen, L., Vitek, M.P., 2007. The tau N279K exon 10 splicing mutation recapitulates frontotemporal dementia and parkinsonism linked to chromosome 17 tauopathy in a mouse model. J. Neurosci. 27, 9155–9168.
Gabbott, P.L., Warner, T.A., Jays, P.R., Salway, P., Busby, S.J., 2005. Prefrontal cortex in the rat: projections to subcortical autonomic, motor, and limbic centers. J. Comp. Neurol. 492, 145–177.
Goedert, M., Spillantini, M.G., Jakes, R., Rutherford, D., Crowther, R.A., 1989. Multiple isoforms of human microtubule-associated protein tau: sequences and localization in neurofibrillary tangles of Alzheimer's disease. Neuron 3, 519–526.
Gotz, J., Probst, A., Spillantini, M.G., Schafer, T., Jakes, R., Burki, K., Goedert, M., 1995. Somatodendritic localization and hyperphosphorylation of tau protein in transgenic mice expressing the longest human brain tau isoform. EMBO J. 14, 1304–1313.
Hanger, D.P., Betts, J.C., Loviny, T.L., Blackstock, W.P., Anderton, B.H., 1998. New phosphorylation sites identified in hyperphosphorylated tau (paired helical filament-tau) from Alzheimer's disease brain using nanoelectrospray mass spectrometry. J. Neurochem. 71, 2465–2476.
Hanger, D.P., Byers, H.L., Wray, S., Leung, K.Y., Saxton, M.J., Seereeram, A., Reynolds, C.H., Ward, M.A., Anderton, B.H., 2007. Novel phosphorylation sites in tau from Alzheimer brain support a role for casein kinase 1 in disease pathogenesis. J. Biol. Chem. 282, 23645–23654.
Hanger, D.P., Anderton, B.H., Noble, W., 2009. Tau phosphorylation: the therapeutic challenge for neurodegenerative disease. Trends Mol. Med. 15, 112–119.
Ikeda, M., Shoji, M., Kawarai, T., Kawarabayashi, T., Matsubara, E., Murakami, T., Sasaki, A., Tomidokoro, Y., Ikarashi, Y., Kuribara, H., Ishiguro, K., Hasegawa, M., Yen, S.H., Chishti, M.A., Harigaya, Y., Abe, K., Okamoto, K., St George-Hyslop, P., Westaway, D., 2005. Accumulation of filamentous tau in the cerebral cortex of human tau R406W transgenic mice. Am. J. Pathol. 166, 521–531.
Iqbal, K., Grundke-Iqbal, I., 2008. Alzheimer neurofibrillary degeneration: significance, etiopathogenesis, therapeutics and prevention. J. Cell. Mol. Med. 12, 38–55.
Iqbal, K., Grundke-Iqbal, I., Zaidi, T., Merz, P.A., Wen, G.Y., Shaikh, S.S., Wisniewski, H.M., Alafuzoff, I., Winblad, B., 1986. Defective brain microtubule assembly in Alzheimer's disease. Lancet 2, 421–426.
Iqbal, K., Braak, E., Braak, H., Zaidi, T., Grundke-Iqbal, I., 1991. A silver impregnation method for labeling both Alzheimer paired helical filaments and their polypeptides separated by sodium dodecyl sulfate-polyacrylamide gel electrophoresis. Neurobiol. Aging 12, 357–361.
Ishihara, T., Hong, M., Zhang, B., Nakagawa, Y., Lee, M.K., Trojanowski, J.Q., Lee, V.M., 1999. Age-dependent emergence and progression of a tauopathy in transgenic mice overexpressing the shortest human tau isoform. Neuron 24, 751–762.
Ishihara, T., Zhang, B., Higuchi, M., Yoshiyama, Y., Trojanowski, J.Q., Lee, V.M., 2001. Age-dependent induction of congophilic neurofibrillary tau inclusions in tau transgenic mice. Am. J. Pathol. 158, 555–562.
Ittner, L.M., Fath, T., Ke, Y.D., Bi, M., van Eersel, J., Li, K.M., Gunning, P., Gotz, J., 2008. Parkinsonism and impaired axonal transport in a mouse model of frontotemporal dementia. Proc. Natl. Acad. Sci. USA 105, 15997–16002.
Jameson, L., Frey, T., Zeeberg, B., Dalldorf, F., Caplow, M., 1980. Inhibition of microtubule assembly by phosphorylation of microtubule-associated proteins. Biochemistry 19, 2472–2479.
Jeganathan, S., Hascher, A., Chinnathambi, S., Biernat, J., Mandelkow, E.M., Mandelkow, E., 2008. Proline-directed pseudo-phosphorylation at AT8 and PHF1 epitopes induces a compaction of the paperclip folding of Tau and generates a pathological (MC-1) conformation. J. Biol. Chem. 283, 32066–32076.
Kalivas, P.W., Nakamura, M., 1999. Neural systems for behavioral activation and reward. Curr. Opin. Neurobiol. 9, 223–227.
Kenessey, A., Yen, S.H., 1993. The extent of phosphorylation of fetal tau is comparable to that of PHF-tau from Alzheimer paired helical filaments. Brain Res. 629, 40–46.
Kimura, T., Yamashita, S., Fukuda, T., Park, J.M., Murayama, M., Mizoroki, T., Yoshiike, T., Sahara, N., Takashima, A., 2007. Hyperphosphorylated tau in parahippocampal cortex impairs place learning in aged mice expressing wild-type human tau. EMBO J. 26, 5143–5152.
Kojima, N., Ishibashi, H., Okada, K., Kandel, E.R., 1998. Higher seizure susceptibility and enhanced tyrosine phosphorylation of N-methyl-D-aspartate receptor subunit 2B in fyn transgenic mice. Learn. Mem. 5, 429–445.
Lambourne, S.L., Humby, T., Isles, A.R., Emson, P.C., Spillantini, M.G., Wilkinson, L.S., 2007. Impairments in impulse control in mice transgenic for the human FTDP-17 tauV337M mutation are exacerbated by age. Hum. Mol. Genet. 16, 1708–1719.
Lee, V.M., Goedert, M., Trojanowski, J.Q., 2001. Neurodegenerative tauopathies. Annu. Rev. Neurosci. 24, 1121–1159.
Lewis, J., McGowan, E., Rockwood, J., Melrose, J., Nacharaju, P., Van Slegtenhorst, M., Gwinn-Hardy, K., Paul Murphy, M., Yu, X., Duff, K., Hardy, J., Corral, A., Lin, W.L., Yen, S.H., Dickson, D.W., Davies, P., Hutton, M., 2000. Neurofibrillary tangles, amyotrophy and progressive motor disturbance in mice expressing mutant (P301L) tau protein. Nat. Genet. 25, 402–405.
Lindwall, G., Cole, R.D., 1984. Phosphorylation affects the ability of tau protein to promote microtubule assembly. J. Biol. Chem. 259, 5301–5305.
Martinez, G., Ropero, C., Funes, A., Flores, E., Blotta, C., Landa, A.I., Gargiulo, P.A., 2002. Effects of selective NMDA and non-NMDA blockade in the nucleus accumbens on the plus-maze test. Physiol. Behav. 76, 219–224.
Mizuma, H., Shukuri, M., Hayashi, T., Watanabe, Y., Onoe, H., 2010. Establishment of in vivo brain imaging method in conscious mice. J. Nucl. Med. 51, 1068–1075.
Mogensen, J., Divac, I., 1993. Behavioural changes after ablation of subdivisions of the rat prefrontal cortex. Acta Neurobiol. Exp. (Wars) 53, 439–449.
Morgane, P.J., Galler, J.R., Mokler, D., 2005. A review of systems and networks of the limbic forebrain/limbic midbrain. Prog. Neurobiol. 75, 143–160.
Morishima-Kawashima, M., Hasegawa, M., Takio, K., Suzuki, M., Yoshida, H., Titani, K., Ihara, Y., 1995a. Proline-directed and non-proline-directed phosphorylation of PHF-tau. J. Biol. Chem. 270, 823–829.
Morishima-Kawashima, M., Hasegawa, M., Takio, K., Suzuki, M., Yoshida, H., Watanabe, A., Titani, K., Ihara, Y., 1995b. Hyperphosphorylation of tau in PHF. Neurobiol. Aging 16, 365–371.
Murakami, T., Paitel, E., Kawarabayashi, T., Ikeda, M., Chishti, M.A., Janus, C., Matsubara, E., Sasaki, A., Kawarai, T., Phinney, A.L., Harigaya, Y., Horne, P., Egashira, N., Mishima, K., Hanna, A., Yang, J., Iwasaki, K., Takahashi, M., Fujiwara, M., Ishiguro, K., Bergeron, C., Carlson, G.A., Abe, K., Westaway, D., St George-Hyslop, P., Shoji, M., 2006. Cortical neuronal and glial pathology in TgTauP301L transgenic mice: neuronal degeneration, memory disturbance, and phenotypic variation. Am. J. Pathol. 169, 1365–1375.
Pennartz, C.M., Groenewegen, H.J., Lopes da Silva, F.H., 1994. The nucleus accumbens as a complex of functionally distinct neuronal ensembles: an integration of behavioural, electrophysiological and anatomical data. Prog. Neurobiol. 42, 719–761.
Polydoro, M., Acker, C.M., Duff, K., Castillo, P.E., Davies, P., 2009. Age-dependent impairment of cognitive and synaptic function in the htau mouse model of tau pathology. J. Neurosci. 29, 10741–10749.
Probst, A., Gotz, J., Wiederhold, K.H., Tolnay, M., Mistl, C., Jaton, A.L., Hong, M., Ishihara, T., Lee, V.M., Trojanowski, J.Q., Jakes, R., Crowther, R.A., Spillantini, M.G., Burki, K., Goedert, M., 2000. Axonopathy and amyotrophy in mice transgenic for human four-repeat tau protein. Acta Neuropathol. 99, 469–481.
Ramsden, M., Kotilinek, L., Forster, C., Paulson, J., McGowan, E., SantaCruz, K., Guimaraes, A., Yue, M., Lewis, J., Carlson, G., Hutton, M., Ashe, K.H., 2005. Age-dependent neurofibrillary tangle formation, neuron loss, and memory impairment in a mouse model of human tauopathy (P301L). J. Neurosci. 25, 10637–10647.
Rocher, A.B., Chapon, F., Blaizot, X., Baron, J.C., Chavoiz, C., 2003. Resting-state brain glucose utilization as measured by PET is directly related to regional synaptophysin levels: a study in baboons. Neuroimage 20, 1894–1898.
Sahara, N., Lewis, J., DeTure, M., McGowan, E., Dickson, D.W., Hutton, M., Yen, S.H., 2002. Assembly of tau in transgenic animals expressing P301L tau: alteration of phosphorylation and solubility. J. Neurochem. 83, 1498–1508.
Sahara, N., Maeda, S., Murayama, M., Suzuki, T., Dohmae, N., Yen, S.H., Takashima, A., 2007. Assembly of two distinct dimers and higher-order oligomers from full-length tau. Eur. J. Neurosci. 25, 3020–3029.
Santacruz, K., Lewis, J., Spires, T., Paulson, J., Kotilinek, L., Ingelsson, M., Guimaraes, A., DeTure, M., Ramsden, M., McGowan, E., Forster, C., Yue, M., Orne, J., Janus, C., Mariash, A., Kuskowski, M., Hyman, B., Hutton, M., Ashe, K.H., 2005. Tau suppression in a neurodegenerative mouse model improves memory function. Science 309, 476–481.
Sargolini, F., Florian, C., Oliverio, A., Mele, A., Roullet, P., 2003. Differential involvement of NMDA and AMPA receptors within the nucleus accumbens in consolidation of information necessary for place navigation and guidance strategy of mice. Learn. Mem. 10, 285–292.
Schindowski, K., Bretteville, A., Leroy, K., Begard, S., Brion, J.P., Hamdane, M., Buee, L., 2006. Alzheimer's disease-like tau neuropathology leads to memory deficits and loss of functional synapses in a novel mutated tau transgenic mouse without any motor deficits. Am. J. Pathol. 169, 599–616.
Schoenbaum, G., Setlow, B., Ramus, S.J., 2003. A systems approach to orbitofrontal cortex function: recordings in rat orbitofrontal cortex reveal interactions with different learning systems. Behav. Brain Res. 146, 19–29.
Spires, T.L., Orne, J.D., SantaCruz, K., Pitstick, R., Carlson, G.A., Ashe, K.H., Hyman, B.T., 2006. Region-specific dissociation of neuronal loss and neurofibrillary pathology in a mouse model of tauopathy. Am. J. Pathol. 168, 1598–1607.
Spittaels, K., Van den Haute, C., Van Dorpe, J., Bruynseels, K., Vandezande, K., Laenen, I., Geerts, H., Mercken, M., Sciot, R., Van Lommel, A., Loos, R., Van

Leuven, F., 1999. Prominent axonopathy in the brain and spinal cord of transgenic mice overexpressing four-repeat human tau protein. Am. J. Pathol. 155, 2153–2165.
Stanford, P.M., Brooks, W.S., Teber, E.T., Hallupp, M., McLean, C., Halliday, G.M., Martins, R.N., Kwok, J.B., Schofield, P.R., 2004. Frequency of tau mutations in familial and sporadic frontotemporal dementia and other tauopathies. J. Neurol. 251, 1098–1104.
Tanemura, K., Murayama, M., Akagi, T., Hashikawa, T., Tominaga, T., Ichikawa, M., Yamaguchi, H., Takashima, A., 2002. Neurodegeneration with tau accumulation in a transgenic mouse expressing V337M human tau. J. Neurosci. 22, 133–141.
Uylings, H.B., Groenewegen, H.J., Kolb, B., 2003. Do rats have a prefrontal cortex? Behav. Brain Res. 146, 3–17.
Wray, S., Saxton, M., Anderton, B.H., Hanger, D.P., 2008. Direct analysis of tau from PSP brain identifies new phosphorylation sites and a major fragment of N-terminally cleaved tau containing four microtubule-binding repeats. J. Neurochem. 105, 2343–2352.
Yoshida, H., Ihara, Y., 1993. Tau in paired helical filaments is functionally distinct from fetal tau: assembly incompetence of paired helical filament-tau. J. Neurochem. 61, 1183–1186.
Yu, Y., Run, X., Liang, Z., Li, Y., Liu, Y., Iqbal, K., Grundke-Iqbal, I., Gong, C.X., 2009. Developmental regulation of tau phosphorylation, tau kinases, and tau phosphatases. J. Neurochem. 108, 1480–1494.
Zamboni, G., Huey, E.D., Krueger, F., Nichelli, P.F., Grafman, J., 2008. Apathy and disinhibition in frontotemporal dementia: Insights into their neural correlates. Neurology 71, 736–742.

Biochemical and Biophysical Research Communications 417 (2012) 116–121

Contents lists available at SciVerse ScienceDirect

Biochemical and Biophysical Research Communications

journal homepage: www.elsevier.com/locate/ybbrc

Epitope mapping of antibodies against TDP-43 and detection of protease-resistant fragments of pathological TDP-43 in amyotrophic lateral sclerosis and frontotemporal lobar degeneration

Hiroshi Tsuji [a,b], Takashi Nonaka [a], Makiko Yamashita [a], Masami Masuda-Suzukake [a], Fuyuki Kametani [a], Haruhiko Akiyama [c], David M.A. Mann [d], Akira Tamaoka [b], Masato Hasegawa [a,*]

[a] Department of Neuropathology and Cell Biology, Tokyo Metropolitan Institute of Medical Science, 2-1-6 Kamikitazawa, Setagaya-ku, Tokyo 156-8506, Japan
[b] Department of Neurology, Graduate School of Comprehensive Human Sciences, University of Tsukuba, 1-1-1 Tenodai, Tsukuba-City, Ibaraki 305-8576, Japan
[c] Dementia Research Project, Tokyo Metropolitan Institute of Medical Science, 2-1-6 Kamikitazawa, Setagaya-ku, Tokyo 156-0057, Japan
[d] Mental Health and Neurodegeneration Research Group, Greater Manchester Neuroscience Centre, University of Manchester, Hope Hospital, Salford M6 8HD, UK

ARTICLE INFO

Article history:
Received 8 November 2011
Available online 22 November 2011

Keywords:
Aggregation
Tau
Alpha-synuclein
ALS
FTLD

ABSTRACT

TAR DNA-binding protein of 43 kDa (TDP-43) is the major component of the intracellular inclusions in amyotrophic lateral sclerosis (ALS) and frontotemporal lobar degeneration (FTLD). Here, we show that both monoclonal (60019-2-Ig) and polyclonal (10782-2-AP) anti-TDP-43 antibodies recognize amino acids 203–209 of human TDP-43. The monoclonal antibody labeled human TDP-43 by recognizing Glu204, Asp205 and Arg208, but failed to react with mouse TDP-43. The antibodies stained the abnormally phosphorylated C-terminal fragments of 24–26 kDa in addition to normal TDP-43 in ALS and FTLD brains. Immunoblot analysis after protease treatment demonstrated that the epitope of the antibodies (residues 203–209) constitutes part of the protease-resistant domain of TDP-43 aggregates which determine a common characteristic of the pathological TDP-43 in both ALS and FTLD-TDP. The antibodies and methods used in this study will be useful for the characterization of abnormal TDP-43 in human materials, as well as in vitro and animal models for TDP-43 proteinopathies.

1. Introduction

TDP-43 is a nuclear ribonucleoprotein implicated in exon splicing, gene transcription, regulation of mRNA stability, mRNA biosynthesis, and formation of nuclear bodies [1–5]. It has been identified as the major component of the ubiquitin-positive tau-negative intracytoplasmic inclusions in frontotemporal lobar degeneration (FTLD), amyotrophic lateral sclerosis (ALS) [6,7] and other neurodegenerative disorders [8–12]. Identification of mutations in familial and sporadic ALS and FTLD cases demonstrated a direct link between the genetic lesion and development of TDP-43 pathology [13–16]. Immunohistochemical studies using anti-TDP-43 antibodies revealed that TDP-43 translocates from its normal nuclear localization into the cytoplasm in these disorders. Furthermore, biochemical analysis detected abnormally phosphorylated TDP-43 of 45 kDa, high-molecular-weight smearing and C-terminal fragments of approximately 25 kDa, as well as normal TDP-43 of 43 kDa in the detergent-insoluble, urea-soluble fraction from affected brains. The antibodies generated by immunizing C-terminal phosphopeptides of TDP-43, such as pS409/410 and pS403/404, strongly stain abnormal neuronal cytoplasmic and dendritic inclusions in FTLD, and skein-like and glial cytoplasmic inclusions in ALS spinal cord, with no nuclear staining, and thus permit easier and more sensitive detection of abnormal TDP-43 accumulations in neuropathological examination [17]. Immunoblotting of the Sarkosyl-insoluble fractions from FTLD and ALS cases using these phosphospecific antibodies clearly demonstrated that hyperphosphorylated full-length TDP-43 of 45 kDa, smearing substances and fragments at 18–26 kDa are the major species of TDP-43 accumulated in FTLD and ALS, and the band patterns of the C-terminal fragments of phosphorylated TDP-43 correspond to the neuropathological subtypes.

Anti-TDP-43 monoclonal antibody (mAb) (60019-2-Ig; Proteintech Group Inc., Chicago, IL) and polyclonal antibody (pAb) (10782-2-AP; Proteintech Group Inc., Chicago, IL) are widely used for the investigation of TDP-43 pathology [6,7,9,18–21]. According to the manufacturer's specifications, anti-TDP-43 mAb and pAb were generated against the N-terminal 260 amino acids (aa) of the protein, but the precise epitope has not yet been identified. Another mouse monoclonal antibody against TDP-43 (2E2-D3; Abnova Corporation, Taipei, Taiwan) is also commercially available; it recognizes residues 205–222 of human TDP-43, but does not recognize mouse or rat TDP-43 [22].

* Corresponding author. Fax: +81 3 6834 2349.
E-mail address: hasegawa-ms@igakuken.or.jp (M. Hasegawa).

0006-291X/$ - see front matter © 2011 Elsevier Inc. All rights reserved.
doi:10.1016/j.bbrc.2011.11.066

In this study, we mapped the epitope for anti-TDP-43 mAb and pAb (Proteintech Group Inc.). We also showed that anti-TDP-43 mAb recognizes human TDP-43, but not mouse TDP-43. Using these antibodies, we investigated the abnormal forms of TDP-43 from ALS and FTLD brains, and found that the antibodies recognized the amino-terminus of the TDP-43 C-terminal fragments of 24–26 kDa. Immunoblot analysis of Sarkosyl-insoluble fractions after treatment of proteases also demonstrated that the epitope is apparently resistant to trypsin and chymotrypsin in the abnormal TDP-43, suggesting that the epitope region is important for the formation of the pathological structure of TDP-43 in ALS and FTLD.

2. Materials and methods

2.1. Construction of plasmids

GFP-tagged TDP-43 C-terminal or N-terminal fragments were constructed as described [23] by amplifying a cDNA encoding full-length TDP-43 by means of PCR and inserting the fragment into the pEGFP-C1 vector (Clontech). To investigate the specificity of TDP-43 mAb for human TDP-43, site-directed mutagenesis of GFP-tagged full-length TDP-43 was carried out to substitute Glu204 to Ala (E204A), Asp205 to Glu (D205E), Arg208 to Gln (R208Q), Glu209 to Gln (E209Q), Ser212 to Cys (S212C), Asp216 to Glu (D216E), and Met218 to Val (M218V), using a site-directed mutagenesis kit (Strategene)(Fig. 4). All constructs were verified by DNA sequencing.

2.2. Antibodies

TDP-43 polyclonal antibody, 10782-2-AP, and TDP-43 monoclonal antibody, 60019-2-Ig, were purchased from Proteintech Group Inc. Anti-GFP monoclonal antibody was purchased from MBL (Nagoya, Japan). A polyclonal antibody specific for phosphorylated TDP-43 (pS409/410) was prepared as described [17].

2.3. Cell culture and expression of plasmids

Human neuroblastoma cell line SH-SY5Y and mouse neuroblastoma cell line Neuro 2a were maintained in appropriate medium as described previously [24,25]. Cells were then transfected with expression plasmids using FuGENE6 (Roche) according to the manufacturer's instructions.

2.4. Immunoblotting

Expressed proteins in cell lysates were separated by 10% SDS–PAGE and transferred onto polyvinylidene difluoride membrane (Millipore, Bedford, MA). After blocking with 3% gelatin, membranes were incubated overnight with primary antibodies (1:1000) at room temperature. After incubation with an appropriate biotinylated secondary antibody, labeling was detected using the ABC system (Vector Lab., Burlingame, CA) coupled with a diaminobenzidine (DAB) reaction intensified with nickel chloride.

2.5. Analysis of abnormal TDP-43 in ALS and FTLD-TDP brain

Brains from two cases with Alzheimer's disease (AD), two with ALS, two with FTLD-TDP (type A), two with FTLD-TDP (type B) and two with FTLD-TDP (type C) were employed in this study. The two AD cases had no TDP-43 pathology. The age, sex, brain weight, and diagnosis are given in Table 1. Sarkosyl-insoluble, urea-soluble fractions were extracted from these brains as previously described [6,9]. The samples were loaded onto 15% polyacrylamide gel and transferred onto a membrane. The membrane was cut in the center of the loaded lane, and the same samples were reacted separately with anti-TDP-43 Abs and pS409/410 as described above.

Table 1
Description of subjects.

Case No.	Diagnosis	Age (years)	Sex	BW (g)
1	AD	65	F	1165
2	AD	70	F	1126
3	ALS	62	M	1230
4	ALS	42	F	1140
5	FTLD-TDP (type A)	71	F	863
6	FTLD-TDP (type A)	66	F	1100
7	FTLD-TDP (type B)	45	M	1260
8	FTLD-TDP (type B)	67	M	1280
9	FTLD-TDP (type C)	67	M	na
10	FTLD-TDP (type C)	59	M	na

BW, brain weight; AD, Alzheimer's disease; ALS, amyotrophic lateral sclerosis; FTLD-TDP, frontotemporal lobar degeneration with TDP-43 pathology; na, not available.

2.6. Protease treatment of TDP-43

Sarkosyl-insoluble fractions extracted from neocortical regions of the brains were treated with trypsin (at a final concentration of 100 μg/ml, Promega, Madison, USA) or chymotrypsin (at a concentration of 10 μg/ml, Sigma–Aldrich, St. Louis, USA) at 37 °C for 30 min. The reaction was stopped by boiling for 5 min. After centrifuging at 15,000 rpm for 1 min, the samples were analyzed by immunoblotting with anti-TDP-43 pAb and mAb as described above.

3. Results

3.1. Epitope mapping of anti-TDP-43 antibody

Our previous study showed that both TDP-43 mAb and pAb reacted with GFP-tagged TDP-43 C-terminal fragment (GFP-TDP 162–414), but failed to detect GFP-TDP 218–414 [23]. To map the epitope of these antibodies, we expressed a series of GFP-tagged human TDP-43 C-terminal fragments (Fig. 1A) in SH-SY5Y cells and immunoblotted them with the antibodies. Both anti-TDP-43 pAb and mAb detected endogenous human TDP-43 of 43 kDa and exogenous GFP-tagged full-length, 171–414, 181–414, 191–414 and 201–414 TDP-43. However, both antibodies failed to detect 211–414 (Fig. 1A). These results suggest that the epitopes of these antibodies are located within residues 201–210.

To narrow down the epitope structure further, another series of GFP-tagged C-terminal fragments of TDP-43 was expressed in SH-SY5Y cells (Fig. 1B) and tested. Both antibodies reacted with GFP-TDP 203–414, but failed to recognize GFP-TDP 204–414, 205–414 and 207–414 (Fig. 1B), demonstrating that Thr203 forms the N-terminal border of the epitope for both antibodies.

To determine the C-terminus of the epitope, a series of GFP-tagged N-terminal fragments of TDP-43 was expressed and immunoblotted with these antibodies (Fig 1C). Anti-TDP-43 pAb reacted with all of the N-terminal fragments tested, although it stained the 1-212 fragment most strongly. This suggests that one of the pAb epitopes is located at the N-terminal region of TDP-43, in addition to the central epitope. Anti-TDP-43 mAb strongly stained GFP-TDP 1-212, moderately stained GFP-TDP 1-210, and barely stained GFP-TDP 1-209, while it failed to react with GFP 1-208 and 1-207 (Fig. 1C), indicating that Glu209 forms the C-terminus of the epitope for anti-TDP-43 mAb. Thus, anti-TDP-43 mAb recognizes residues 203–209 of human TDP-43.

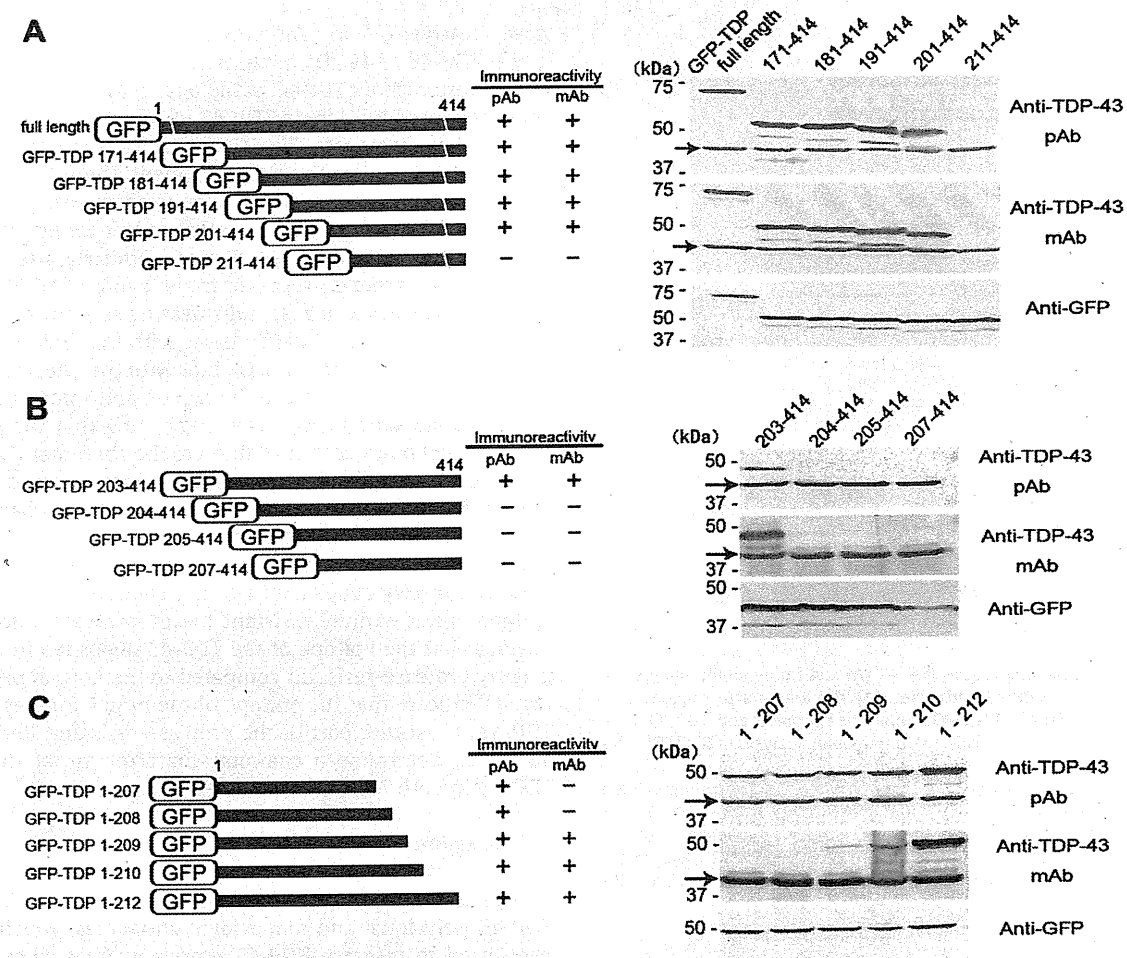

Fig. 1. Epitope mapping of anti-TDP-43 polyclonal and monoclonal antibodies. (A) Schematic diagram of GFP-tagged full-length TDP-43 (GFP-TDP) and the C-terminal fragments. Immunoblot analyses of GFP-TDP and the C-terminal fragments in SH-SY5Y cells. Both mAb and pAb reacted with GFP-TDP and the C-terminal fragments, except for 211–414. The anti-GFP antibody recognizes all the proteins expressed. (B) Further epitope mapping of anti-TDP-43 antibodies. Immunoblot analyses of the GFP tagged C-terminal fragments of TDP-43. Both mAb and pAb reacted with 203–414, but failed to recognize 204–414, 205–414, and 207–414. The anti-GFP antibody recognizes all of the fragments. (C) Epitope mapping of the C-terminus recognized by anti-TDP-43 polyclonal and monoclonal antibodies. Immunoblot analyses of GFP-TDP and N-terminal fragments in SH-SY5Y cells. Anti-TDP-43 pAb reacted with all of the N-terminal fragments, although it stained 1-212 fragment most strongly. In contrast, anti-TDP-43 mAb strongly stained GFP-TDP 1-212, moderately stained GFP-TDP 1-210, and barely stained GFP-TDP 1-209, while it failed to react with GFP 1-208 and 1-207. The anti-GFP antibody recognized all of the fragments equally. The arrows indicate endogenous TDP-43 in SH-SY5Y cells.

3.2. Amino acid sequence differences between human and mouse TDP-43

The anti-TDP-43 mAb reacted with endogenous TDP-43 of human neuroblastoma SH-SY5Y cells, but not with TDP-43 of mouse neuroblastoma Neuro2a cells (Fig. 1B, 1C, 2B). Similarly, the mAb recognized TDP-43 in human brain extract, but failed to detect TDP-43 in mouse brain extract, suggesting that the mAb does not recognize mouse TDP-43 (data not shown). The absence of reactivity with mouse TDP-43 is explained by the sequence differences around the epitope between human and mouse TDP-43 (Fig. 2A). Each different amino acid of human TDP-43 was substituted to that of mouse TDP-43. The mutated proteins were expressed in Neuro2a cells and immunoreactivity with anti-TDP-43 mAb was examined. Substitution of D216 to E and M218 to V did not affect the immunoreactivity (Fig. 2B), whereas substitutions of E204 to A, D205 to E, and R208 to Q abolished the immunoreactivity of anti-TDP-43 mAb, indicating that these residues are necessary for recognition by the mAb. Anti-TDP-43 pAb reacted with these mutants, although a marked decrease in immunoreactivity was observed in the cases of E204A, D205A, R208Q, and S212C.

3.3. Biochemical analysis of abnormal TDP-43 in ALS and FTLD brains with anti-TDP-43 mAb

On immunoblots of Sarkosyl-insoluble fractions extracted from the brain of patients with ALS and FTLD-TDP (type A), the anti-TDP-43 mAb detected phosphorylated full-length TDP-43 at 45 kDa, two bands around 25 kDa and high-molecular-weight smears, in addition to the normal TDP-43 band at 43 kDa, which can also be detected in control cases. Immunoblot analysis of the split membrane with a phosphorylation-dependent anti-TDP-43 antibody pS409/410 revealed that the two bands around 25 kDa stained with the mAb corresponded to the C-terminal fragments of 24 and 26 kDa recognized by pS409/410 (Fig. 3)[17]. These results demonstrated that these 24 and 26 kDa C-terminal fragments contain the epitope of the mAb, residues 203–209, and that the cleavage sites of these C-terminal fragments are located at the N-terminal side of Thr203.

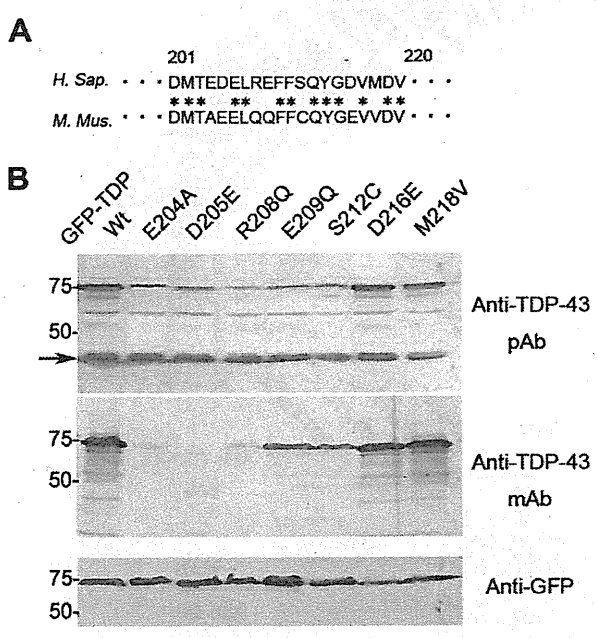

Fig. 2. Alignment of human and mouse TDP-43 (A) and immunoblot analyses of mutated TDP-43 with anti-TDP-43 antibodies. (A) The amino acid sequences of human (upper) and mouse (lower) TDP-43 around the epitope of anti-TDP-43 mAb. The asterisks show identical amino acids. (B) Immunoblot analyses of GFP-TDP wild type (Wt) and GFP-TDP mutants expressed in Neuro2a cells. Substitution of D216 to E and M218 to V did not affect the immunoreactivity, whereas substitutions of E204 to A, D205 to E, and R208 to Q, abolished the immunoreactivity of anti-TDP-43 mAb. Anti-TDP-43 pAb reacted with all these mutants, although markedly decreased immunoreactivities were observed in E204A, D205A, R208Q, and S212C. The arrows indicated endogenous TDP-43 in Neuro2A cells. Note that endogenous mouse TDP-43 in Neuro 2a cells was not recognized by anti-TDP-43 mAb.

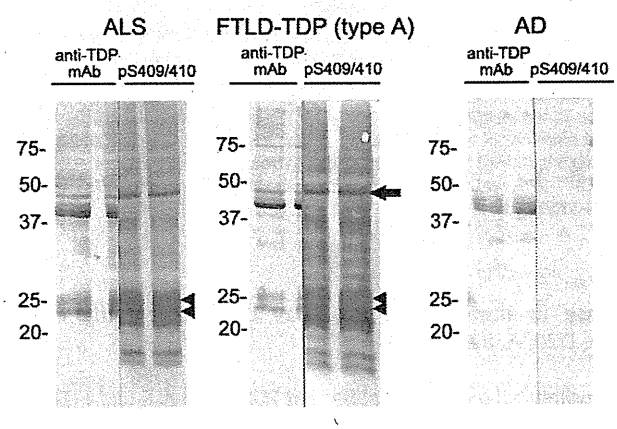

Fig. 3. Immunoblot analyses of Sarkosyl-insoluble fractions from ALS, FTLD-TDP (type A), and AD brains with anti-TDP-43 monoclonal antibody and phosphorylation-dependent anti-TDP-43 antibody, pS409/410. With pS409/410, fragments of approximately 45 kDa and 18–26 kDa, as well as smearing, were detected. The banding pattern of 18–26 kDa fragments showed three major bands at 23, 24, and 26 kDa, and 2 minor bands at 18 and 19 kDa, with the 24 kDa band being the most intense. In addition to the normal full-length TDP-43 at 43 kDa, anti-TDP-43 mAb labeled phosphorylated full-length TDP-43 at 45 kDa, high-molecular-weight smears and two bands at 26 kDa and 24 kDa (arrowheads), which were not seen in the AD case. The two bands corresponded to the major 26 and 24 kDa bands were detected with pS409/410.

3.4. The epitope of these TDP-43 antibodies constitute part of protease-resistant core domain of TDP-43 in ALS and FTLD brains

In order to characterize the epitope further, we treated the Sarkosyl-insoluble fractions extracted from brains of patients with proteases and analyzed them with these antibodies. Without protease treatment, both antibodies strongly stained normal full-length TDP-43 of 43 kDa in all cases examined including AD cases which were without TDP-43 pathology. In ALS and FTLD-TDP cases, phosphorylated full-length TDP-43 of 45 kDa (Fig 4A, arrows) and the ~25 kDa fragments (Fig 4A, arrow heads) were detected with these antibodies. After trypsin treatment, the full-length band of TDP-43 was disappeared and the protease-resistant fragments around 25 kDa (Fig 4B, white arrows) and smearing substances appeared in the ALS and FTLD-TDP cases. Similarly, after chymotrypsin treatment, protease-resistant triplet bands of 16, 20 and 25 kDa (Fig 4C, white arrow heads) and smearing substances were clearly detected in ALS and FTLD-TDP-cases with the mAb, while no such bands were seen in AD cases. On blot with the pAb, multiple bands were detected in addition to the triplet, and some of these bands were also detected in AD cases, suggesting that the pAb stained some normal fragments in addition to the abnormal TDP-43 bands. In the cases examined, apparent difference was not detected in these trypsin-resistant and chymotrypsin-resistant bands detected among the clinicopathological phenotypes of the diseases. By proteinase K treatment, immunoreactivities with these antibodies were completely abolished (data not shown), suggesting that the epitope is not entirely resistant to any proteases. However, it is obvious that the epitope of the TDP-43 deposited in the patients is fairly protease-resistant compared to the normal protein. These results indicate that the epitope of the mAb (residues 203–209 of TDP-43) constitute part of the protease-resistant domain of TDP-43 which determine a common characteristic of the abnormal TDP-43 in both ALS and FTLD-TDP.

4. Discussion

This is the first analysis of the epitopes of Proteintech's anti-TDP-43 polyclonal and monoclonal antibodies, which have often been used to research TDP-43 proteinopathies since 2006 [6,7]. We demonstrated that anti-TDP-43 mAb specifically recognizes residues 203–209 of human TDP-43, which form a part of the second RNA-recognition motif (RRM2, residues 193–257) of normal TDP-43 [26], but constitute part of the protease-resistant core domain of TDP-43 aggregates that determine the common characteristic of abnormal TDP-43 in ALS and FTLD-TDP-43.

RRM2 is a functional domain with distinct RNA/DNA binding characteristics. The anti-TDP-43 mAb recognized human TDP-43, but not mouse TDP-43. Site-directed mutagenesis and subsequent immunoblot analysis revealed that Glu204, Asp205 and Arg208 residues in human TDP-43 are important for the specific recognition by the mAb (Fig. 2). In fact, human TDP-43 shares 98.5% homology with mouse TDP-43 at the amino acid level, but the RRM2 domain has only 66% homology.

We also showed that one of the major epitopes of the pAb is located in almost the same region at that of the mAb (Fig. 1), although the pAb also recognizes the N-terminal region of TDP-43. Recently, TDP-43 transgenic mice overexpressing human TDP-43 have been produced as animal models of TDP-43 proteinopathy [27]. However, abnormal TDP-43 pathologies in these mice are very rare, so new transgenic or other animal models that develop abundant TDP-43 pathology are still required. Since the TDP-43 mAb recognizes human TDP-43, but not mouse TDP-43, it will be a useful reagent for the characterization of mouse lines transgenic for human TDP-43, together with phosphorylation-dependent antibodies.

Biochemical analyses of TDP-43 proteinopathies have demonstrated that abnormally phosphorylated full-length and C-terminal fragments of TDP-43 are the major species in the inclusions. The band patterns of the C-terminal fragments at 18–26 kDa are closely correlated with the clinicopathological subtypes of TDP-43 proteinopathies [17]. In addition, most of the pathogenic mutations

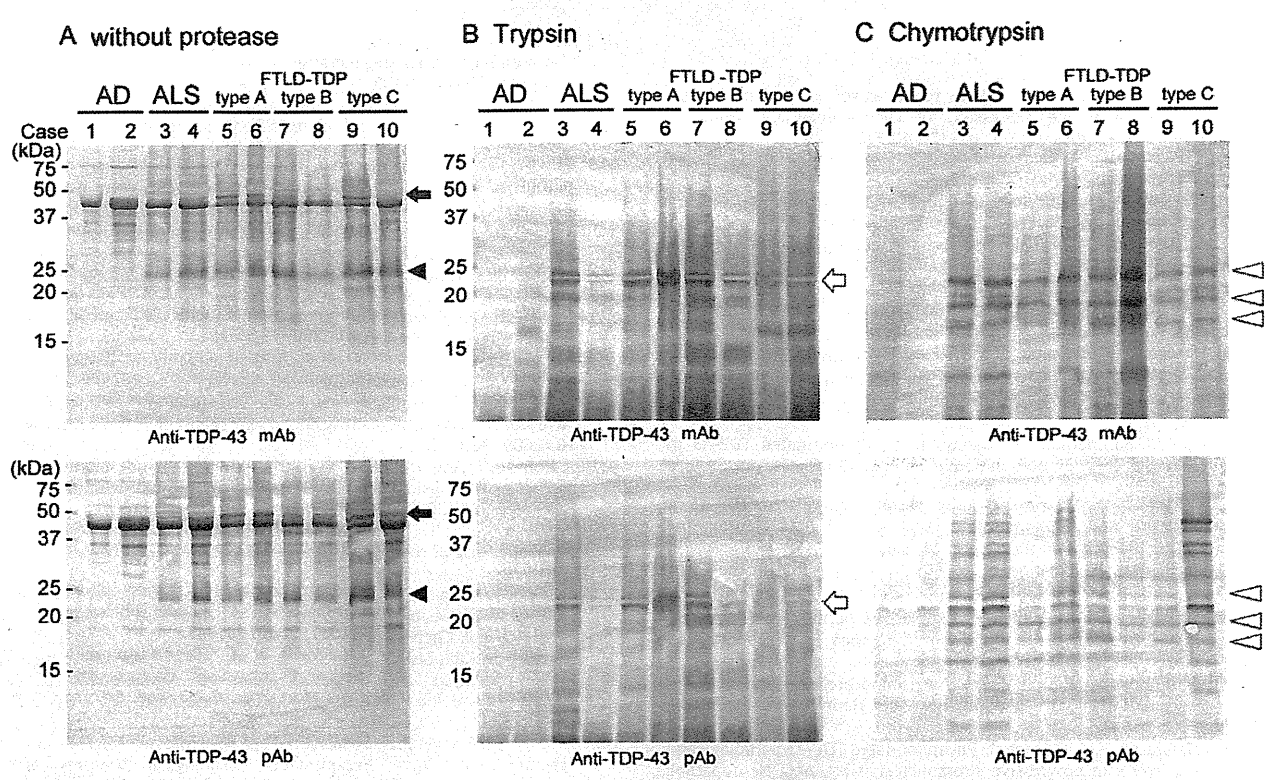

Fig. 4. Immunoblot analysis of Sarkosyl-insoluble fractions from AD and TDP-43 proteinopathies before and after protease treatment. (A) Without protease treatment, normal TDP-43 of 43 kDa was detected with these antibodies in all cases examined. In the ALS and FTLD-TDP cases, phosphorylated full-length TDP-43 of 45 kDa (arrows), high-molecular-weight smears, and the 24–26 kDa fragments (arrow heads) were detected in addition to the normal TDP-43. (B) Upon trypsin treatment, full-length TDP-43 disappeared, and the protease-resistant ~25 kDa fragments (white arrows) and smears appeared in ALS and FTLD-TDP cases, but not in AD cases. (C) After chymotrypsin treatment, triplet bands (white arrowheads) were detected in ALS and FTLD-TDP cases with the mAb and multiple bands were detected with pAb, whereas such immunoreactivities were hardly detected in AD cases.

are found in the C-terminal half of the TDP-43 [13–16]. Therefore, misfolding or structural alteration of the C-terminal half of TDP-43 seems to be the key to the pathogenesis of TDP-43 proteinopathies. By mass spectrometric analysis of the 23 kDa band in Sarkosyl-insoluble fraction from FTLD-TDP (type A), we identified the cleavage site as the N-terminus of Asp219 [23]. Another group reported cleavage at Asp208, based on N-terminal sequencing of urea extracts of FTLD-TDP brain [28]. However, the cleavage sites of the other major C-terminal fragments of 24 and 26 kDa have not been determined yet. In this study, we showed that the pathological TDP-43 C-terminal fragments of 24 and 26 kDa in ALS and FTLD-TDP type A contain the epitope of anti-TDP-43 mAb, residues 203–209, by comparing the immunoblotting results with those using pS409/410 (Fig. 3). This result suggests that the cleavage sites of pathological TDP-43 C-terminal fragments in ALS and FTLD-TDP are located at the N-terminal side of Thr203. Although the mechanisms of generation of the C-terminal fragments are still controversial, the presence of multiple cleavage sites suggests that cleavage may occur after the aggregation or assembly of TDP-43.

Structural or conformational changes in the proteins are thought to be the most important in protein aggregation in these neurodegenerative diseases. To analyze the conformational change in the epitope of TDP-43 from normal to the abnormal states further, we treated the Sarkosyl-insoluble TDP-43 with trypsin or chymotrypsin, and immunoblotted with these antibodies. The protease-resistant TDP-43 bands and smears were detected in ALS and all subtypes of FTLD-TDP with these anti-TDP-43 antibodies (Fig. 4), while no such bands were seen in AD cases. These demonstrate that the epitope is protease-resistant in the abnormal TDP-43 but not in normal TDP-43. Using an antibody pS409/410 that recognizes the C-terminal phosphorylation sites, some protease-resistant TDP-43 bands are detected, and the band patterns are slightly different between ALS and FTLD-TDP type C [29]. On immunoblots with anti-TDP-43 pAb and mAb, such difference was not observed. This is probably due to that the epitope of the mAb and pAb is located in the amino-terminus of the protease-resistant core of the TDP-43, whereas epitope of the pS409/410 located in the C-terminus. Similar protease-resistant bands have been reported in abnormal prion in prion diseases, tau in Alzheimer's disease and alpha-synuclein in Parkinson's disease and dementia with Lewy bodies. Biochemical studies in these proteinopathies suggested that the protease-resistant bands represent the core domains of the filamentous aggregates of these proteins with cross-β structures [30–32]. By analogy with these proteins we propose that these protease-resistant C-terminal fragments represent the core of the filamentous aggregates of TDP-43. Since the epitope of the mAb and pAb are determined to locate at residues 203–209, this may be important in the formation of a core region of pathological TDP-43 aggregates which is common in all TDP-43 proteinopathies. Finally, the protease treatment used in this study may be useful for detection of the abnormal TDP-43 in brains of patients, animal models, culture cells and in vitro models with these anti-TDP-43 antibodies more specifically, as used for detection of abnormal prion proteins.

Acknowledgments

Authors thank Dr Tetsuaki Arai (Tsukuba University) for helpful advice and discussions. This work was supported by a Grant-in-Aid for Scientific Research (A) (to M.H., 11000624) from Ministry of Education, Culture, Sports, Science and Technology of Japan, and grants from Ministry of Health, Labor and Welfare of Japan (to M.H.).

References

[1] Y.M. Ayala, T. Misteli, F.E. Baralle, TDP-43 regulates retinoblastoma protein phosphorylation through the repression of cyclin-dependent kinase 6 expression, Proc. Natl. Acad. Sci. U.S.A. 105 (2008) 3785–3789.

[2] Y.M. Ayala, F. Pagani, F.E. Baralle, TDP43 depletion rescues aberrant CFTR exon 9 skipping, FEBS Lett. 580 (2006) 1339–1344.

[3] E. Buratti, F.E. Baralle, Multiple roles of TDP-43 in gene expression, splicing regulation, and human disease, Front. Biosci. 13 (2008) 867–878.

[4] S.H. Ou, F. Wu, D. Harrich, et al., Cloning and characterization of a novel cellular protein, TDP-43, that binds to human immunodeficiency virus type 1 TAR DNA sequence motifs, J. Virol. 69 (1995) 3584–3596.

[5] I.F. Wang, N.M. Reddy, C.K. Shen, Higher order arrangement of the eukaryotic nuclear bodies, Proc. Natl. Acad. Sci. U.S.A. 99 (2002) 13583–13588.

[6] T. Arai, M. Hasegawa, H. Akiyama, et al., TDP-43 is a component of ubiquitin-positive tau-negative inclusions in frontotemporal lobar degeneration and amyotrophic lateral sclerosis, Biochem. Biophys. Res. Commun. 351 (2006) 602–611.

[7] M. Neumann, D.M. Sampathu, L.K. Kwong, et al., Ubiquitinated TDP-43 in frontotemporal lobar degeneration and amyotrophic lateral sclerosis, Science 314 (2006) 130–133.

[8] T. Arai, I.R. Mackenzie, M. Hasegawa, et al., Phosphorylated TDP-43 in Alzheimer's disease and dementia with Lewy bodies, Acta Neuropathol. (Berl) 117 (2009) 125–136.

[9] M. Hasegawa, T. Arai, H. Akiyama, et al., TDP-43 is deposited in the Guam parkinsonism-dementia complex brains, Brain 130 (2007) 1386–1394.

[10] C.F. Tan, M. Yamada, Y. Toyoshima, et al., Selective occurrence of TDP-43-immunoreactive inclusions in the lower motor neurons in Machado-Joseph disease, Acta Neuropathol. (Berl) 118 (2009) 553–560.

[11] Y. Toyoshima, H. Tanaka, M. Shimohata, et al., Spinocerebellar ataxia type 2 (SCA2) is associated with TDP-43 pathology, Acta Neuropathol. (Berl) 122 (2011) 375–378.

[12] O. Yokota, Y. Davidson, E.H. Bigio, et al., Phosphorylated TDP-43 pathology and hippocampal sclerosis in progressive supranuclear palsy, Acta Neuropathol. (Berl) 120 (2010) 55–66.

[13] E. Kabashi, P.N. Valdmanis, P. Dion, et al., TARDBP mutations in individuals with sporadic and familial amyotrophic lateral sclerosis, Nat. Genet. 40 (2008) 572–574.

[14] J. Sreedharan, I.P. Blair, V.B. Tripathi, et al., TDP-43 mutations in familial and sporadic amyotrophic lateral sclerosis, Science 319 (2008) 1668–1672.

[15] A. Tamaoka, M. Arai, M. Itokawa, et al., TDP-43 M337V mutation in familial amyotrophic lateral sclerosis in Japan, Intern. Med. 49 (2010) 331–334.

[16] I.R. Mackenzie, R. Rademakers, M. Neumann, TDP-43 and FUS in amyotrophic lateral sclerosis and frontotemporal dementia, Lancet Neurol. 9 (2010) 995–1007.

[17] M. Hasegawa, T. Arai, T. Nonaka, et al., Phosphorylated TDP-43 in frontotemporal lobar degeneration and amyotrophic lateral sclerosis, Ann. Neurol. 64 (2008) 60–70.

[18] I.R. Mackenzie, E.H. Bigio, P.G. Ince, et al., Pathological TDP-43 distinguishes sporadic amyotrophic lateral sclerosis from amyotrophic lateral sclerosis with SOD1 mutations, Ann. Neurol. 61 (2007) 427–434.

[19] M. Neumann, L.K. Kwong, A.C. Truax, et al., TDP-43-positive white matter pathology in frontotemporal lobar degeneration with ubiquitin-positive inclusions, J. Neuropathol. Exp. Neurol. 66 (2007) 177–183.

[20] H. Zhang, C.F. Tan, F. Mori, et al., TDP-43-immunoreactive neuronal and glial inclusions in the neostriatum in amyotrophic lateral sclerosis with and without dementia, Acta Neuropathol. (Berl) 115 (2008) 115–122.

[21] M. Neumann, I.R. Mackenzie, N.J. Cairns, et al., TDP-43 in the ubiquitin pathology of frontotemporal dementia with VCP gene mutations, J. Neuropathol. Exp. Neurol. 66 (2007) 152–157.

[22] H.X. Zhang, K. Tanji, F. Mori, et al., Epitope mapping of 2E2-D3, a monoclonal antibody directed against human TDP-43, Neurosci. Lett. 434 (2008) 170–174.

[23] T. Nonaka, F. Kametani, T. Arai, et al., Truncation and pathogenic mutations facilitate the formation of intracellular aggregates of TDP-43, Hum. Mol. Genet. 18 (2009) 3353–3364.

[24] T. Nonaka, T. Arai, E. Buratti, et al., Phosphorylated and ubiquitinated TDP-43 pathological inclusions in ALS and FTLD-U are recapitulated in SH-SY5Y cells, FEBS Lett. 583 (2009) 394–400.

[25] Y. Nishimoto, D. Ito, T. Yagi, et al., Characterization of alternative isoforms and inclusion body of the TAR DNA-binding protein-43, J. Biol. Chem. 285 (2010) 608–619.

[26] E. Buratti, F.E. Baralle, Characterization and functional implications of the RNA binding properties of nuclear factor TDP-43, a novel splicing regulator of CFTR exon 9, J. Biol. Chem. 276 (2001) 36337–36343.

[27] H. Wils, G. Kleinberger, J. Janssens, et al., TDP-43 transgenic mice develop spastic paralysis and neuronal inclusions characteristic of ALS and frontotemporal lobar degeneration, Proc. Natl. Acad. Sci. U.S.A. 107 (2010) 3858–3863.

[28] L.M. Igaz, L.K. Kwong, A. Chen-Plotkin, et al., Expression of TDP-43 C-terminal Fragments in Vitro Recapitulates Pathological Features of TDP-43 Proteinopathies, J. Biol. Chem. 284 (2009) 8516–8524.

[29] M. Hasegawa, T. Nonaka, H. Tsuji, et al., Molecular Dissection of TDP-43 Proteinopathies, J. Mol. Neurosci. 45 (2011) 480–485.

[30] J. Collinge, K.C. Sidle, J. Meads, et al., Molecular analysis of prion strain variation and the aetiology of 'new variant' CJD, Nature 383 (1996) 685–690.

[31] H. Miake, H. Mizusawa, T. Iwatsubo, et al., Biochemical characterization of the core structure of alpha-synuclein filaments, J. Biol. Chem. 277 (2002) 19213–19219.

[32] M. Novak, J. Kabat, C.M. Wischik, Molecular characterization of the minimal protease resistant tau unit of the Alzheimer's disease paired helical filament, EMBO J. 12 (1993) 365–370.

Neurobiology of Disease 45 (2012) 862–870

Contents lists available at SciVerse ScienceDirect

Neurobiology of Disease

journal homepage: www.elsevier.com/locate/ynbdi

Oxidative stress induced by glutathione depletion reproduces pathological modifications of TDP-43 linked to TDP-43 proteinopathies

Yohei Iguchi [a], Masahisa Katsuno [a], Shinnosuke Takagi [a], Shinsuke Ishigaki [a,d], Jun-ichi Niwa [b], Masato Hasegawa [c], Fumiaki Tanaka [a], Gen Sobue [a,d,*]

[a] Department of Neurology, Nagoya University Graduate School of Medicine, 65 Tsurumai-cho, Showa-ku, Nagoya 466–8550, Japan
[b] Stroke Center, Aichi Medical University, Aichi 480–1195, Japan
[c] Departments of Molecular Neurobiology, Tokyo Institute of Psychiatry, Tokyo Metropolitan Organization for Medical Research, 2-1-8 Kamikitazawa, Setagaya-ku, Tokyo 156–8585, Japan
[d] CREST, Japan Science and Technology Agency, 4-1-8, Honcho, Kawaguchi, Saitama 332–0012, Japan

ARTICLE INFO

Article history:
Received 30 March 2011
Revised 29 August 2011
Accepted 4 December 2011
Available online 13 December 2011

Keywords:
TAR DNA-binding protein 43 kDa (TDP-43)
TDP-43 proteinopathy
Oxidative stress
Glutathione depletion
Post-translational modification
Protein phosphorylation

ABSTRACT

TAR DNA-binding protein 43 (TDP-43) is a major component of ubiquitin-positive inclusion of TDP-43 proteinopathies including amyotrophic lateral sclerosis and frontotemporal lobar degeneration with ubiquitinated inclusions, which is now referred to as FTLD-TDP. TDP-43 in the aberrant inclusion is known to be hyperphosphorylated at C-terminal sites, to be truncated at the N-terminal region, and to re-distribute from nucleus to cytoplasm or neurite. The pathogenic role of these modifications, however, has not been clarified. Furthermore, there is no evidence about the initial cause of these modifications. Herein we show that ethacrynic acid (EA), which is able to increase cellular oxidative stress through glutathione depletion, induces TDP-43 C-terminal phosphorylation at serine 403/404 and 409/410, insolubilization, C-terminal fragmentation, and cytoplasmic distribution in NSC34 cells and primary cortical neurons. In the investigation using a nonphosphorylable mutant of TDP-43, there was no evidence that C-terminal phosphorylation of TDP-43 contributes to its solubility or distribution under EA induction. Our findings suggest that oxidative stress induced by glutathione depletion is associated with the process of the pathological TDP-43 modifications and provide new insight for TDP-43 proteinopathies.

Introduction

TAR DNA-binding protein 43 (TDP-43) is a major component of ubiquitin-positive inclusion, a pathological hallmark of TDP-43 proteinopathies including amyotrophic lateral sclerosis (ALS) and frontotemporal lobar degeneration with ubiquitinated inclusions, which is now referred to as FTLD-TDP (Arai et al., 2006; Neumann et al., 2006). Both diseases occur in sporadic or familial forms, and are characterized by late-onset progressive deterioration of motor and/or cognitive function. TDP-43 is a heterogeneous nuclear ribonucleoprotein (hnRNP), which is known to regulate gene transcription and exon splicing through interactions with RNA, hnRNPs, and nuclear bodies (Ayala et al., 2005; Buratti et al., 2005; Wang et al., 2002, 2004). In addition, this protein has also been reported to stabilize human low molecular weight neurofilament (hNFL) mRNA through direct interaction with its 3'UTR (Strong et al., 2007), regulate retinoblastoma protein phosphorylation through the repression of cyclin-dependent kinase 6 (Cdk6) expression (Ayala et al., 2008), regulate activity of Rho family GTPases (Iguchi et al., 2009), and alter the expression of selected microRNAs, such as let-7b and miR-663 (Buratti et al., 2010). Furthermore, very recent works using cross-linking immunoprecipitation sequencing show that multiple RNAs interact with TDP-43 (Polymenidou et al., 2011; Sephton et al., 2011; Tollervey et al., 2011).

Although it mostly localizes in the nucleus under normal conditions, TDP-43 is distributed from nucleus to cytoplasm or neurite, and forms aggregates consisting mainly of C-terminal fragments in affected neurons of patients with TDP-43 proteinopathies. In addition, TDP-43 in the aberrant aggregation is hyperphosphorylated at multiple C-terminal sites (Hasegawa et al., 2008). However, neither the pathogenic role nor the initial cause of these abnormal modifications of TDP-43 has been elucidated. The fact that the majority of patients with TDP-43 proteinopathies are sporadic suggests that exogenous factors induce post-translational modifications of TDP-43 that are seen in the disease. Furthermore, TDP-43 inclusions have also been observed in Alzheimer disease (AD), Parkinson disease (PD),

Abbreviations: TDP-43, TAR DNA-binding protein of 43 kDa; ALS, amyotrophic lateral sclerosis; hnRNP, heterogeneous nuclear ribonucleoprotein; hNFL, human low molecular weight neurofilament; Cdk6, cyclin-dependent kinase 6; ROS, reactive oxygen species; EA, ethacrynic acid; NAC, N-acetylcysteine; CK1, casein kinase 1; CK2, casein kinase 2; WT-TDP-43, wild type TDP-43; SA-TDP-43, nonphosphorylable TDP-43.

* Corresponding author at: Department of Neurology, Nagoya University Graduate School of Medicine, 65 Tsurumai-cho, Showa-ku, Nagoya 466–8550, Japan. Fax: +81 52 744 2785.
E-mail address: sobueg@med.nagoya-u.ac.jp (G. Sobue).

Available online on ScienceDirect (www.sciencedirect.com).

0969-9961/$ – see front matter © 2011 Elsevier Inc. All rights reserved.
doi:10.1016/j.nbd.2011.12.002

dementia with Lewy bodies (DLB), and Huntington disease (HD), argyrophilic grain disease, suggesting that the aggregation of this protein may be a secondary feature of neurodegeneration (Amador-Ortiz et al., 2007; Arai et al., 2009, 2010; Geser et al., 2008; Hasegawa et al., 2007). These findings complicate understanding of the pathogenic role of TDP-43. On the other hand, there is considerable evidence that reactive oxygen species (ROS) and oxidative stress are associated with many neurodegenerative conditions including ALS (Abe et al., 1995, 1997; Beal et al., 1997; Butterfield et al., 2007; Ferrante et al., 1997; Lovell and Markesbery, 2007; Nunomura et al., 2002; Shaw et al., 1995). Herein we show that oxidative stress induced by glutathione depletion reproduces the pathological modifications of TDP-43, that are seen in TDP-43 proteinopathies, in motor neuron-like cells and primary cortical neurons.

Materials and methods

Cell culture and treatment

Mouse NSC34 motor neuron-like cells (a kind gift of N.R. Cashman, University of British Columbia, Vancouver, Canada) were cultured in a humidified atmosphere of 95% air-5% CO2 in a 37 °C incubator in Dulbecco's Modified Eagle's Medium (DMEM) supplemented with 10% fetal bovine serum (FBS). To differentiate the cells, the medium was changed to DMEM containing 1% FBS and 1% NEAA, and was cultured for 24 h. For the interventions, the cells were then incubated with ethacrynic acid (EA) (Sigma-Aldrich, St. Louis, MO), with or without N-acetylcysteine (NAC) (Sigma-Aldrich), casein kinase 1 (CK1) inhibitor (D4476), or casein kinase 2 (CK2) inhibitor (TBCA) (Sigma-Aldrich). Primary cultures of mouse embryonic cortical neurons that were dissociated from embryonic cortex of embryonic day 15 (E15) C57BL/6 J pregnant mice were plated onto poly-L-lysine-coated plates or glass bottom dishes, and maintained in neuron culture medium (Sumilon, Osaka, Japan). Five days after the incubation, the indicated interventions were performed. In both NSC34 cells and primary cortical neurons, the transfections of the intended plasmids were performed using Lipofectamine 2000 (Invitrogen, Eugene, OR), according to the manufacturer's instructions.

DNA constructs

Human wild type TDP-43 (WT-TDP-43) (accession number NM 007375) cDNA was amplified by PCR from cDNA of human spinal cord using the following primers: 5′-CACCATGTCTGAATATATTCGGGTAAC-3′ and 5′-CTACATTCCCCAGCCAGAAGACTTAGAAT-3′. The PCR product was cloned into the pENTR/D-TOPO vector (Invitrogen). For nonphosphorylable TDP-43 (SA-TDP-43) vector, primers containing the mutant substitution of TDP-43 serine 403/404 and 409/410 to alanine were used to mutagenize WT-TDP-43 (KOD-Plus-Mutagenesis kit; Toyobo, Osaka, Japan). The entry vector of WT- or SA-TDP-43 was transferred into pcDNA6.2/N-EmGFP-DEST Vector or pcDNA3.1/nV5-DEST using Gateway LR Clonase II enzyme mix (Invitrogen). The sequences of all constructs were verified using CEQ 8000 genetic analysis system (Beckman Coulter, Brea, CA).

Immunoblot analysis

For whole lysate analysis, NSC34 cells and primary cortical neurons were lysed in 2% SDS sample buffer. For analysis of protein solubility, cells cultured in 6-well plates were lysed in 100 μl of Tris (TS) buffer (50 mM Tris–HCl buffer, pH 7.5, 0.15 M NaCl, 5 mM EDTA, 5 mM EGTA, protein phosphatase inhibitors, and protease inhibitor cocktail). Lysates were sonicated and centrifuged at 100,000 ×g for 15 min. To prevent carryover, the pellets were washed with TS buffer, followed by sonication and centrifugation. TS-insoluble pellets were lysed in 50 μl of Triton-X100 (TX) buffer (TS buffer containing 1% Triton X-100), sonicated, and centrifuged at 100,000 g for 15 min. The pellets were washed with TX buffer, followed by sonication and centrifuge. TX-insoluble pellets were lysed in 50 μl of Sarkosyl (Sar) buffer (TS buffer containing 1% Sarkosyl), sonicated and centrifuged at 100,000 × g for 15 min. Sar-insoluble pellets were lysed in 25 μl of SDS sample buffer. After denaturation, 3 μl of each cell lysate was separated by SDS-PAGE (5%–20% gradient gel) and analyzed by western blotting with ECL Plus detection reagents (GE Healthcare, Buckinghamshire, UK). Primary antibodies used were as follows: anti-TDP-43 rabbit polyclonal antibody (1:1000, ProteinTech, Chicago, IL), anti-TDP-43 (405–414) rabbit polyclonal antibody (1:1000, Cosmo Bio Co. Ltd., Tokyo, Japan), anti-TDP-43 (phospho Ser403/404, Cosmo Bio) rabbit polyclonal antibody (1:1000, Cosmo Bio), anti-TDP-43 (phospho Ser409/410, Cosmo Bio) rabbit polyclonal antibody (1:1000, Cosmo Bio), anti-GAPDH mouse monoclonal antibody (1:2000, Temecula, CA), anti-GFP mouse monoclonal antibody (1:2000, MBL, Nagoya, Japan), and anti-V5 mouse monoclonal antibody (1:2000, Invitrogen).

Assay of ROS production

NSC34 cells to be treated with intended agents were incubated in 96-well plates with 5-(and-6)-chloromethyl-2′,7′-dichlorodihydro fluoresceindiacetate acetyl ester (CM-H2DCFDA) (Molecular Probes, Eugene, OR, USA) for 1 h. Oxidation in the cells was then measured in a multiple-plate reader (PowerscanHT, Dainippon Pharmaceutical, Japan) at excitation and emission wavelengths of 485 nm and 530 nm, respectively. The assays were carried out in 6 wells for each condition.

Immunocytochemistry

NSC34 cells and primary cortical neurons were fixed with 4% paraformaldehyde, incubated with PBS containing 0.2% Triton X-100 for 5 min, blocked, and incubated overnight with anti-TDP-43 rabbit polyclonal antibody (1:1000, ProteinTech), anti-TDP-43 (phospho Ser409/410) mouse monoclonal antibody (1:2000, Cosmo Bio) and anti-TIAR mouse monoclonal antibody (1:1000, BD Transduction Laboratories, Milan, Italy). After washing, samples were incubated with Alexa-488-conjugated goat anti-rabbit IgG (1:1000, Invitrogen) and Alexa-564-conjugated goat anti-mouse IgG (1:1000, Invitrogen) for 30 min, mounted with (Vector Laboratories, Inc. Burlingame, CA), then imaged with a laser conforcal microscope (Nikon A1, Nikon, Tokyo, Japan).

Time lapse analysis

NSC34 cells or mouse primary cortical neurons were grown on glass base dishes, transfected with GFP-WT-TDP-43, and treated with EA. GFP and phase contrast imaging was done every 10 min using a 40X objective lens on a laser scanning confocal microscope.

Cell viability analysis

The 3-(4,5-dimethylthiazol-2-yl)-5-(3-caboxymethoxyphenyl)-2-(4-sulfophenyl)-2H -tetrazolium (MTS)-based cell proliferation assay (MTS assay) was carried out using the CellTiter 96 Aqueous One Solution Cell Proliferation Assay (Promega, Madison, WI), according to the manufacturer's instructions. Absorbance at 490 nm was measured in a multiple-plate reader (PowerscanHT, Dainippon Pharmaceutical, Japan). The assays were carried out in 6 wells for each condition.

Statistical analysis

Statistical differences were analyzed by ANOVA and Bonferroni post hoc analyses for three group comparisons (SPSS version 15.0, SPSS Inc., Chicago, IL). Two-tailed $p<0.05$ was regarded as statistically significant.

Results

EA-mediated oxidative stress induces TDP-43 phosphorylation in NSC34 cells

To investigate the effect of oxidative stress on endogenous TDP-43, NSC34 cells were incubated for 12 h with EA, which is able to increase cellular oxidative stress through depletion of glutathione, (Keelan et al., 2001; Rizzardini et al., 2003). Immunoblots showed abnormal TDP-43-immunoreactive bands at 45 kDa, which suggests hyperphosphorylation of TDP-43, at EA concentration greater than 50 μM EA (Fig. 1A). The bands were immunopositive for phospho-TDP-43-specific (pTDP-43) antibodies at serine 403/404 and serine 409/410 (S403/404 and S409/410), that are seen in TDP-43 proteinopathies as pathological phosphorylation (Hasegawa et al., 2008) (Fig. 1A). In addition, phosphorylation of these TDP-43 sites was prevented by co-treatment with 2 mM NAC, a precursor of glutathione. Quantification of CM-H2DCFDA oxidation, a measure of ROS formation, showed that ROS productions was increased by EA treatment in a dose-dependent manner and was prevented by NAC (Fig. 1B). Since TDP-43 phosphorylation at S403/404 and S409/410 is exerted by CK1 and CK2 (Hasegawa et al., 2008), the effect of treatment with these inhibitors in combination with EA was examined. Both inhibitors prevented serine phosphorylation of TDP-43 in a dose-dependent manner, although CK1 inhibitor was more effective than CK2 inhibitor (Fig. 1C).

EA induces TDP-43 insolubilization and C-terminal fragmentation

To investigate the effect of oxidative stress on endogenous TDP-43 solubility, cells treated with 70 μM EA were extracted sequentially. In the immunoblots, the amount of TDP-43 in TS and TX fractions were significantly decreased, but the amount in Sar and SDS fractions were increased in a time-dependent manner (Fig. 2A). These phenomena were prevented in the presence of 2 mM NAC. Phosphorylated TDP-43 was increased in Sar fractions in a time-dependent manner and was detectable in SDS fractions 5 h after EA induction (Fig. 2A). In addition, long exposure of immunoblots with anti-TDP-43 antibody demonstrated that ~25 kDa C-terminal fragment (CTF) of TDP-43 in Sar and SDS fractions appeared evidently by EA induction, and the amount of TDP-43 CTF in SDS fraction was significantly increased at 5 h after EA induction compared with control (Fig. 2A, B).

EA induces cytoplasmic distribution of TDP-43

Immunocytochemistry showed that endogenous TDP-43 disappeared from the nucleus, translocated to the cytoplasm, and became phosphorylated at least in some population of NSC34 cells treated with 70 μM EA for 5 h, whereas this protein was localized in the nucleus and was not phosphorylated in untreated cells (Fig. 3A). Although the majority of cytoplasmic TDP-43 was diffusely distributed under EA treatment, it was also localized in stress granules (SGs), which were labeled with TIAR (Fig. 3A). The time lapse analysis of NSC43 cells expressing GFP-WT-TDP-43 demonstrated cytoplasmic distribution of TDP-43 in the majority of the cells treated with 70 μM EA, but TDP-43 consistently localized in the nucleus of cells co-treated with 2 mM NAC (Fig. 3B, C).

H_2O_2 induces C-terminal phosphorylation, C-terminal fragmentation, insolubilization, and cytoplasmic distribution of TDP-43

To confirm that the TDP-43 modifications are not induced by the specific toxicity of EA, we investigated the effects of H_2O_2, another

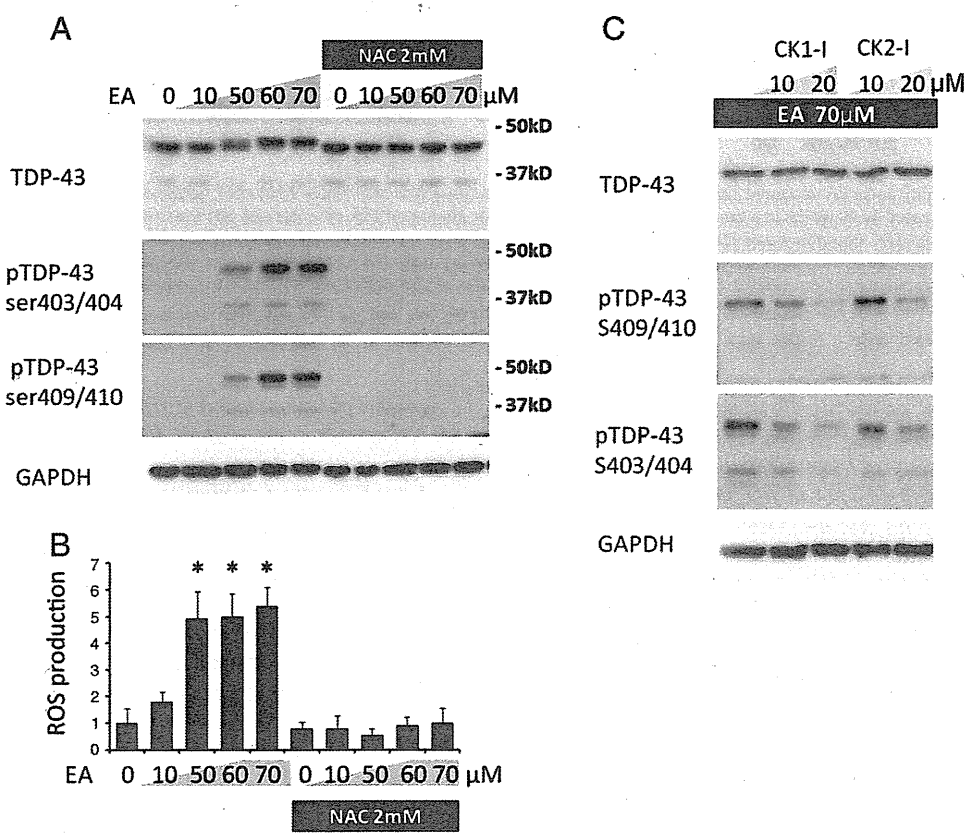

Fig. 1. TDP-43 phosphorylation induced by EA. (A) Immunoblots of NSC34 cells. EA induced TDP-43 C-terminal phosphorylation at S403/404 and S409/410 in a dose-dependent manner. The phosphorylation was prevented by 2 mM NAC. (B) Quantification of ROS by CM-H2DCFDA oxidative assay. The values relative to those of controls are shown. ROS production was increased by EA induction and suppressed by 2 mM NAC. Asterisk denotes significant difference from control ($p<0.0001$, $n=6$). Error bars indicate SD. (C) Immunoblots of NSC34 cells treated with 70 μM of EA. Casein kinase 1 and 2 inhibitors (CK1-I and CK2-I) both prevented the phosphorylation of TDP-43 in a dose-dependent manner.

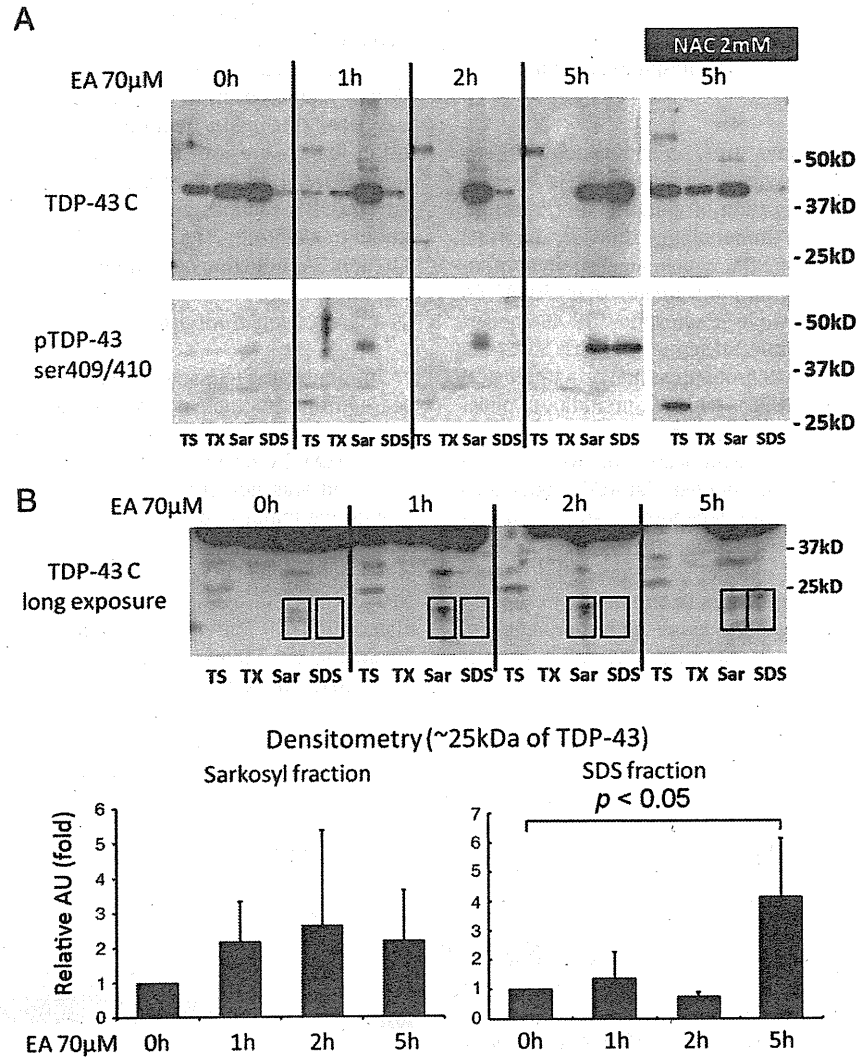

Fig. 2. Analysis of TDP-43 solubility under EA treatment. (A) Sequential extraction analysis using Tris (TS), Triton X100 (TX), Sarkosyl (Sar), and SDS buffers. The amount of TDP-43 in TS and TX fractions was decreased by 70 μM EA in a time-dependent manner, while the amount of TDP-43 in Sar and SDS fractions was increased by the treatment. These phenomena were prevented by 2 mM NAC. Phosphorylated TDP-43 (S409/410) was increased in Sar and SDS fractions in a time-dependent manner. (B) Densitometric quantitation of TDP-43C-terminal fragment (CTF). The relative intensities to controls are shown in arbitrary units (AU). Long exposure of immunoblots with anti-TDP-43 antibody (405–414) (TDP-43C) showed ~25 kDa C-terminal fragment (CTF) in Sar and SDS fractions. The amount of TDP-43 CTF was significantly increased in the SDS fraction at 5 h after EA induction (n = 3). Error bars indicate SD.

inducer of oxidative stress, on the modifications of TDP-43. Immunoblots of NSC34 cells showed that 10 mM H_2O_2 induced C-terminal phosphorylation and C-terminal fragmentation of TDP-43 (Fig. S4A). In the sequential extraction analysis of NSC34 cells, the amount of TDP-43 in TS and TX fractions was decreased by 10 mM H_2O_2, while that of TDP-43 in SDS fraction was increased by the treatment (Fig. S4B). The time lapse analysis of NSC34 cells expressing GFP-WT-TDP-43 showed that 10 mM H_2O_2 induced cytoplasmic distribution of TDP-43 (Fig. S4C).

EA induces C-terminal phosphorylation and cytoplasmic distribution of TDP-43 in primary cortical neurons

To investigate the effect of oxidative stress in neurons, 5-day in vivo (5 DIV) mouse primary cortical neurons were treated with EA for 5 h. Immunoblots showed that EA induced TDP-43 phosphorylation at S403/404 and S409/410 in a dose-dependent manner, and 2 mM NAC prevented the phosphorylation (Fig. 4A). In the time lapse analysis of neurons expressing GFP-WT-TDP-43, TDP-43 was distributed in the cytoplasm in the presence of 30 μM EA (Fig. 4B).

C-terminal phosphorylation of TDP-43 is not mandatory for its insolubilization or cytoplasmic distribution under EA

Since C-terminal phosphorylation of TDP-43 was accompanied by insolubilization and distribution to the cytoplasm in response to oxidative stress, we investigated the effect of C-terminal phosphorylation of TDP-43 using a nonphosphorylable TDP-43 (SA-TDP-43) mutant which contains serine to alanine substitutions at 403/404 and 409/410 (Fig. 5A). We used N-terminal tagged TDP-43, since C-terminal tagged TDP-43 was not detected by anti-pTDP-43 antibody in the immunoblots even under conditions of oxidative stress sufficient to phosphorylate endogenous TDP-43 (Fig. S1). As was seen with WT-TDP-43 under normal conditions, GFP-tagged and V5-tagged SA-TDP-43 were located in the nucleus (Fig. S2). In the immunoblots, endogenous and GFP-WT-TDP-43 were phosphorylated in the presence of 70 μM EA, but GFP-SA-TDP-43 was not phosphorylated even at an EA concentration of 70 μM (Fig. 5B). The time lapse analysis of NSC34 cells demonstrated that GFP-SA-TDP-43 translocated to the cytoplasm (Fig. 6A). The proportion of the cells with cytoplasmic distribution of TDP-43 under oxidative stress was not

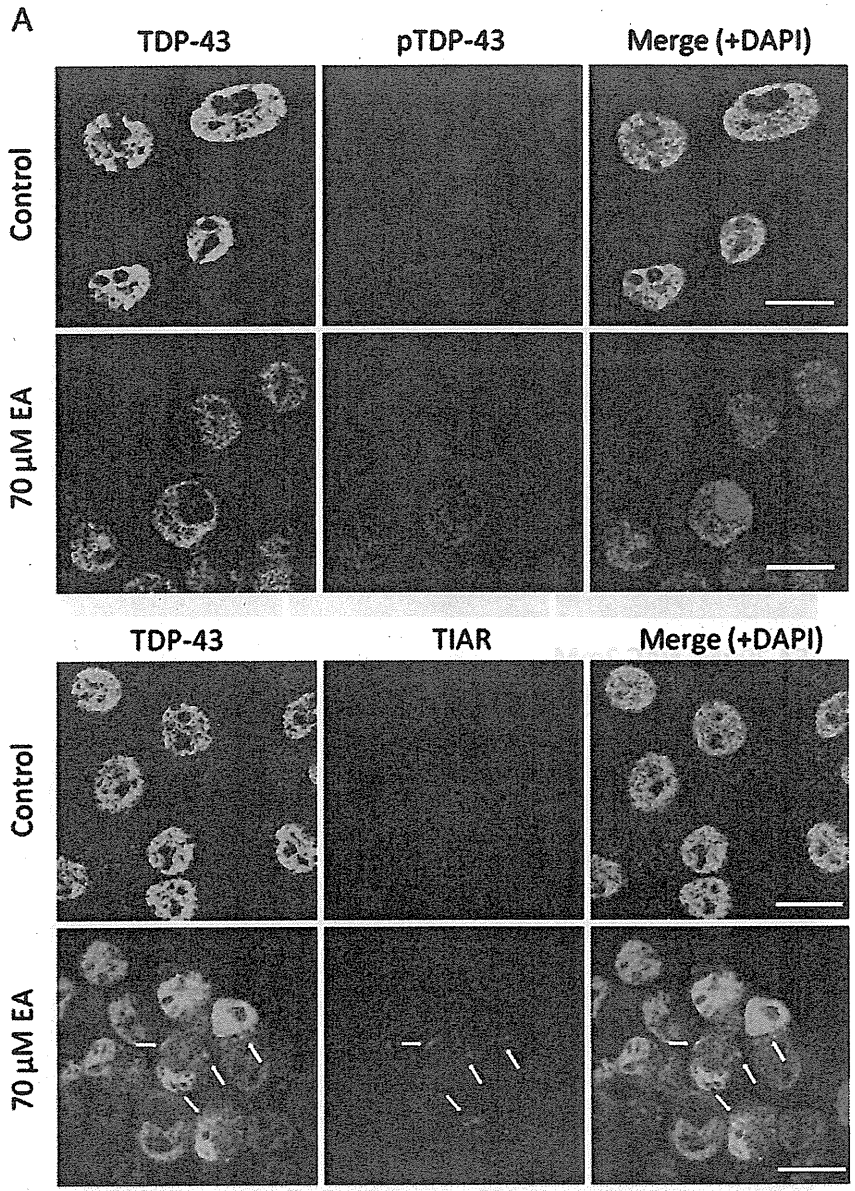

Fig. 3. Cytoplasmic distribution of TDP-43 induced by EA. (A) Immunocytochemistry of NSC34 cells. Cells were stained with anti-TDP-43 antibody (green), anti-phospho-specific TDP-43 (pTDP-43) (S409/410) or anti-TIAR antibody (red), and DAPI (blue). EA treatment (70 μM, 5 h) induced translocation of TDP-43 from the nucleus to the cytoplasm in NSC34 cells. Cytoplasmic TDP-43 was immunopositive for pTDP-43 antibody. In the control cells TDP-43 localized in the nucleus without phosphorylation. TDP-43 co-localized with stress granule marker, TIAR under EA treatment, although the majority of cytoplasmic TDP-43 was diffusely distributed. Arrows indicate stress granules. Scale bars represent 10 μm. (B) Time lapse analysis of NSC43 cells expressing GFP-WT-TDP-43. GFP and phase contrast images showed that TDP-43 was distributed to the cytoplasm when exposed to 70 μM EA, but this distribution was prevented by 2 mM of NAC. (C) The proportion of cells with cytoplasmic distribution of TDP-43 (cells with cyto-TDP) in the GFP-TDP-43 expressing cells 0 h or 5 h after EA induction without or with NAC treatment. Three areas per sample were measured. Error bars indicate SD.

different between WT- and SA-TDP-43 (Fig. 6B). Sequential extraction of NSC34 cells was performed using V5-tagged TDP-43 vectors, since the Sar-insoluble fraction of GFP-TDP-43 was abundant even in the absence of oxidative stress (data not shown). The amount of Sar-insoluble fraction of SA-TDP-43 detected was the same as was seen with WT-TDP-43. (Fig. 7A, B). These findings indicate that phosphorylation is not necessary for oxidative-stress mediated insolubilization and cytoplasmic distribution of TDP-43. Next, we performed MTS assay of NSC34 cells to investigate the effect of TDP-43 and its modifications on the cell viability. The results showed that no significant difference in the viability among the cells expressing GFP-mock, GFP-WT- and GFP-SA-TDP-43, either 0 h or 5 h after EA induction (Fig. S3).

Discussion

Post-translational modifications of TDP-43 such as C-terminal phosphorylation, insolubilization, C-terminal fragmentation, and cytoplasmic distribution are pathological hallmarks of TDP-43 proteinopathies (Arai et al., 2006; Hasegawa et al., 2008; Neumann et al., 2006). TDP-43 with defective nuclear localization signal (NLS) was shown to promote cytoplasmic aggregation, C-terminal phosphorylation, and C-terminal fragmentation of TDP-43 in cell-based studies (Nonaka et al., 2009a; Winton et al., 2008). In addition, overexpression of TDP-43 CTF lead to phosphorylation and formation of cytoplasmic aggregates (Igaz et al., 2009; Nonaka et al., 2009b). Although these observations suggest that the cytoplasmic localization

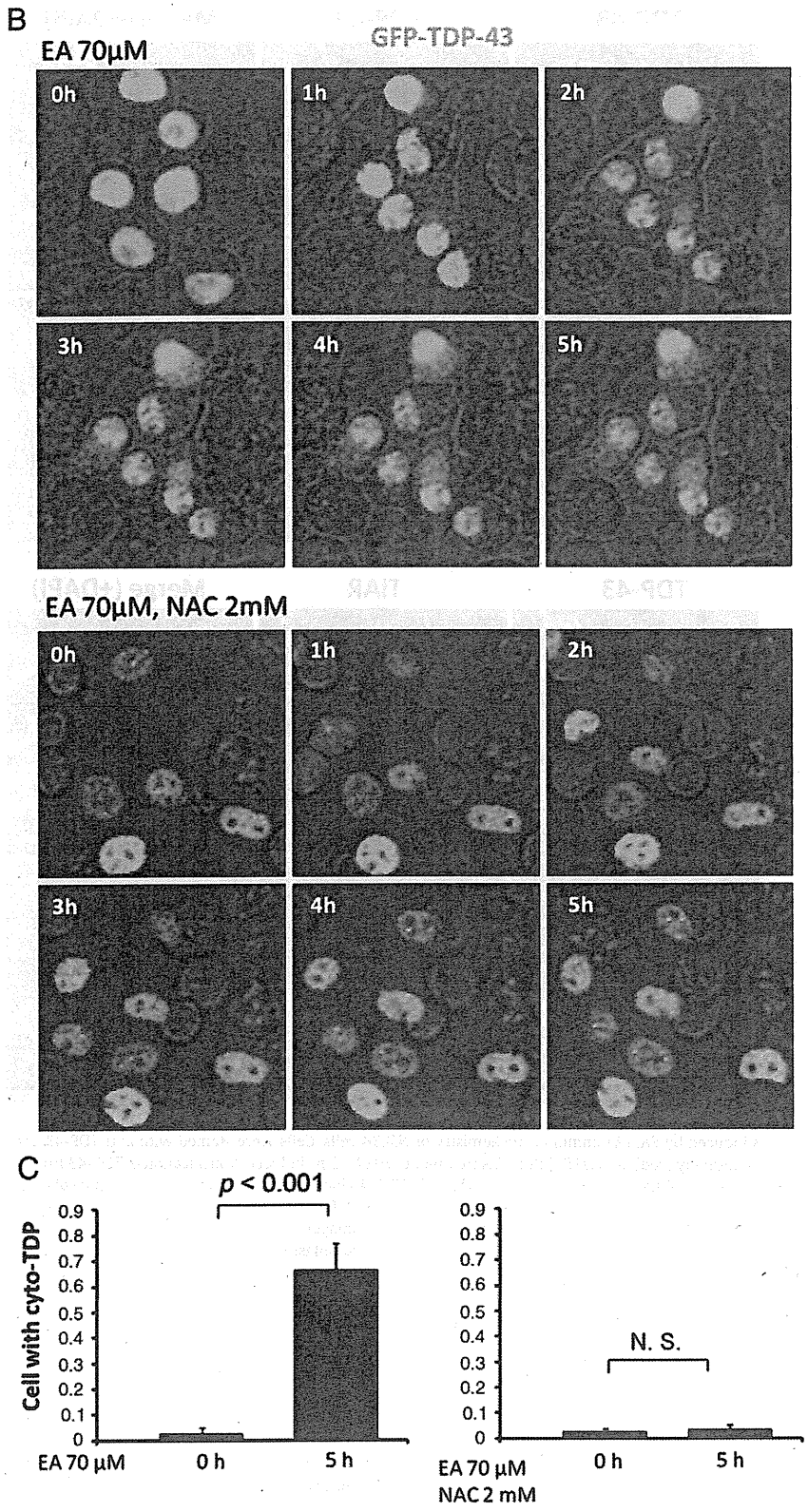

Fig. 3 (*continued*).

or fragmentation of TDP-43 facilitates its pathological modification such as aggregation and phosphorylation, the initial cause of these modifications in TDP-43 proteinopathies has not been fully elucidated. Some studies have demonstrated that artificial axonal damage induces transient cytoplasmic distribution of TDP-43 in motor neurons (Moisse et al., 2009; Sato et al., 2009), indicating that the pathological distribution of TDP-43 may result from the cellular response to neuronal injury or axonal obstruction. However, in these affected neurons, aggregation, C-terminal fragmentation and phosphorylation of TDP-43 were not observed. Furthermore, zinc-induced nuclear

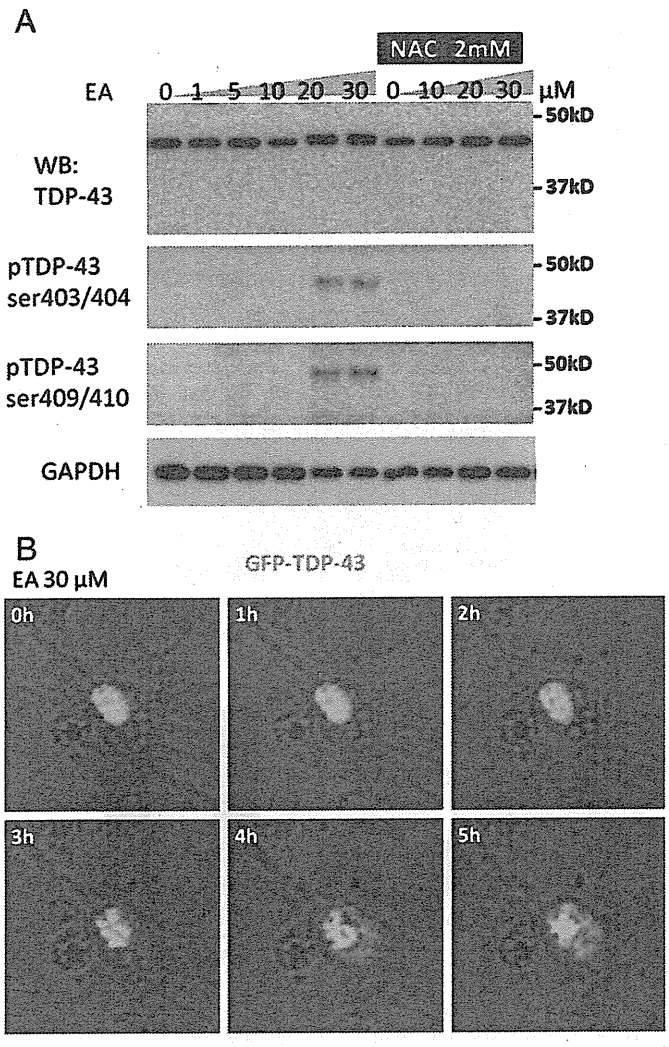

Fig. 4. TDP-43 modification induced by EA in primary cortical neuron. (A) Immunoblots of primary cortical neurons. EA induced TDP-43 phosphorylation at S403/404 and S409/410 in a dose-dependent manner, and this was prevented by 2 mM NAC. (B) Time lapse analysis of neurons expressing GFP-WT-TDP-43. TDP-43 in primary cultures was distributed to the cytoplasm in the presence of 30 μM EA.

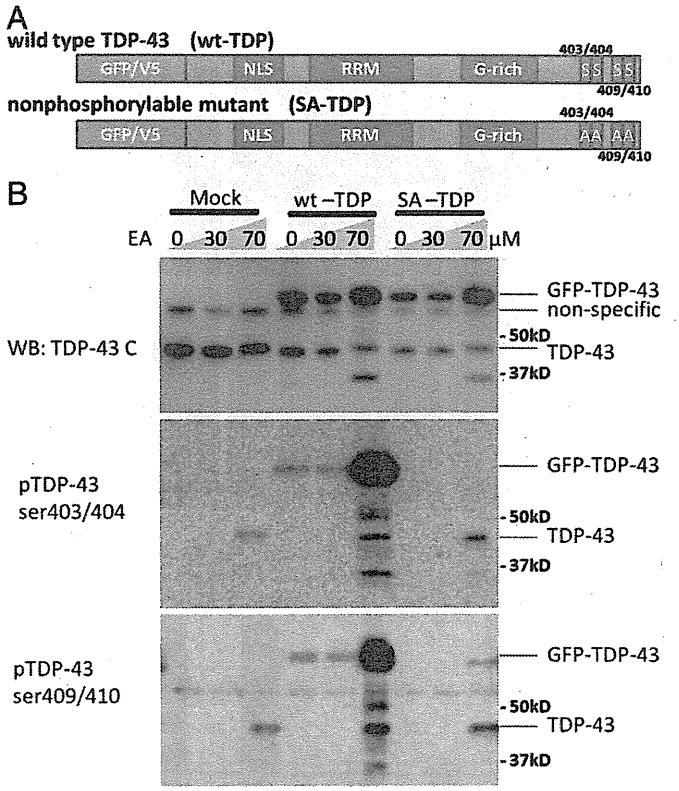

Fig. 5. Nonphosphorylable mutant of TDP-43. (A) Structures of WT- and SA-TDP-43 vectors. SA-TDP-43 contains serine to alanine substitutions at 403/404 and 409/410. (B) Immunoblots of NSC34 cells expressing GFP-WT- or GFP-SA-TDP-43. Endogenous and GFP-WT-TDP-43 were phosphorylated at both 403/404 and 409/410 by 70 μM EA, but GFP-SA-TDP-43 was not phosphorylated by the treatment.

inclusion formations have also been observed in SY5Y cells, but not C-terminal fragmentation or phosphorylation of TDP-43 (Caragounis et al., 2010).

In the present study, we demonstrated that a compound that induces cellular glutathione depletion, EA induced C-terminal phosphorylation of TPD-43 at S403/404 and S409/410 in NSC34 cells and mouse primary cortical neurons, and that NAC completely prevented this phosphorylation. In addition, inhibitors of both CK1 and CK2 also prevented the phosphorylation in a dose-dependent manner. These findings indicate that C-terminal phosphorylation of TDP-43 occurs as a consequence of oxidative stress induced by glutathione depletion and is mediated by CK1 and CK2. Furthermore, the sequential extract analysis showed that EA reduced the solubility of TDP43 and increased the amount of ~25 kDa CTF in the Sar-insoluble fraction. Additionally, EA also induced cytoplasmic distribution of TDP-43 in NSC34 cells and primary cortical neurons. The time lapse analysis showed that cytoplasmic distribution of TDP-43 was seen in the majority of NSC34 cells. Although the immunocytochemistry of TDP-43 demonstrated that cytoplasmic distribution of TDP-43 were observed only in a certain population of NSC34 cells treated with EA, this is likely due to the fact that most of damaged cells could not stay adherent to the plate during the fixation. Previous reports indicated that severe level of oxidative stress may result in apoptotic cell death, and that caspase activation induces C-terminal fragmentation of TDP-43 (Dormann et al., 2009; Zhang et al., 2007). These observations do not exclude the possibility that caspase activation contributes to TDP-43 modifications that were observed under EA treatment. The results of the present study demonstrated that H_2O_2, another inducer of oxidative stress, also causes C-terminal phosphorylation, fragmentation, insolubilization, and cytoplasmic distribution of TDP-43 as observed under EA exposure. These data suggest that oxidative stress is involved in the process of the pathological TDP-43 modifications seen in TDP-43 proteinopathies. The facts that oxidative stress is associated with aging-related disorders (Frederickson et al., 2005; Migliore, 2005) and that TDP-43 proteinopathies are aging process-related diseases may support our assumption that oxidative stress possibly mediates TDP-43 modification. A high frequency of abnormal TDP-43 pathology such as C-terminal phosphorylation has been found not only in patients with TDP-43 proteinopathies but also in patients with other neurodegenerative disease such as AD, DLB, and HD (Arai et al., 2010). Since numerous studies have demonstrated increased oxidative cellular damage in these conditions (Butterfield et al., 2007; Lovell and Markesbery, 2007; Nunomura et al., 2002), oxidative stress may be a cause of pathological TDP-43 modification in various neurodegenerative disorders.

Several studies demonstrated that TDP-43 is involved in SGs under cellular stresses including arsenite treatment and heat shock (Colombrita et al., 2009; Liu-Yesucevitz et al., 2010; McDonald et al., 2011; Nishimoto et al., 2010). Although TDP-43 was seen as a component of SGs under EA treatment, majority of cytoplasmic TDP-43 was independent of SGs and was diffusely distributed. These findings suggest that there is SG-independent mechanism for cytoplasmic distribution of TDP-43 under oxidative stress induced by glutathione depletion.

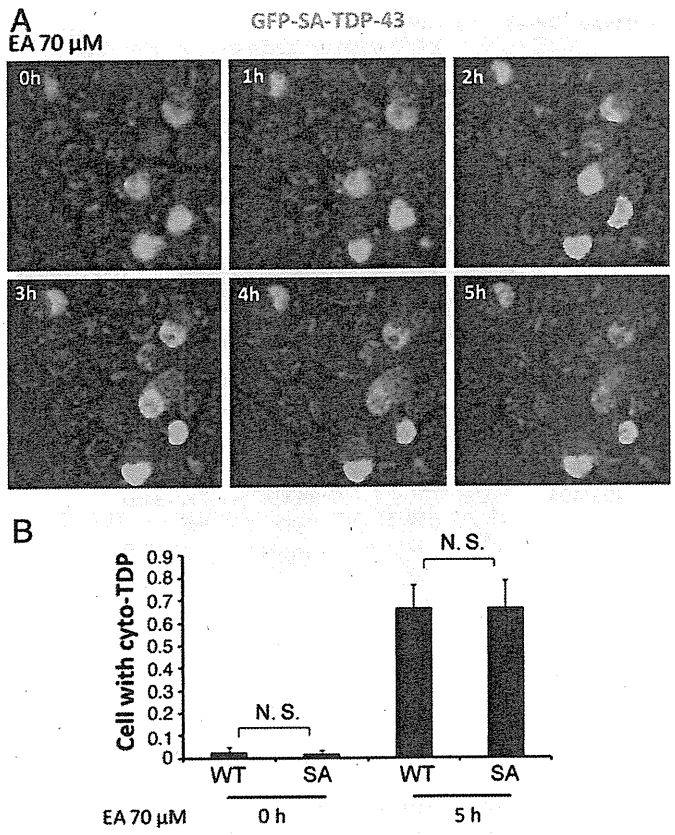

Fig. 6. The effect of C-terminal phosphorylation on TDP-43 distribution. (A) Time lapse analysis of NSC34 cells expressing GFP-SA-TDP-43. GFP-SA-TDP-43 was distributed to the cytoplasm by 70 μM of EA. (B) The proportion of cells with cytoplasmic distribution of TDP-43 (cells with cyto-TDP) in the GFP-TDP-43 expressing cells. The proportion of cells with cyto-TDP was not different between WT- and SA-TDP-43, either 0 h or 5 h after EA induction. Three areas per sample were measured. Error bars indicate SD.

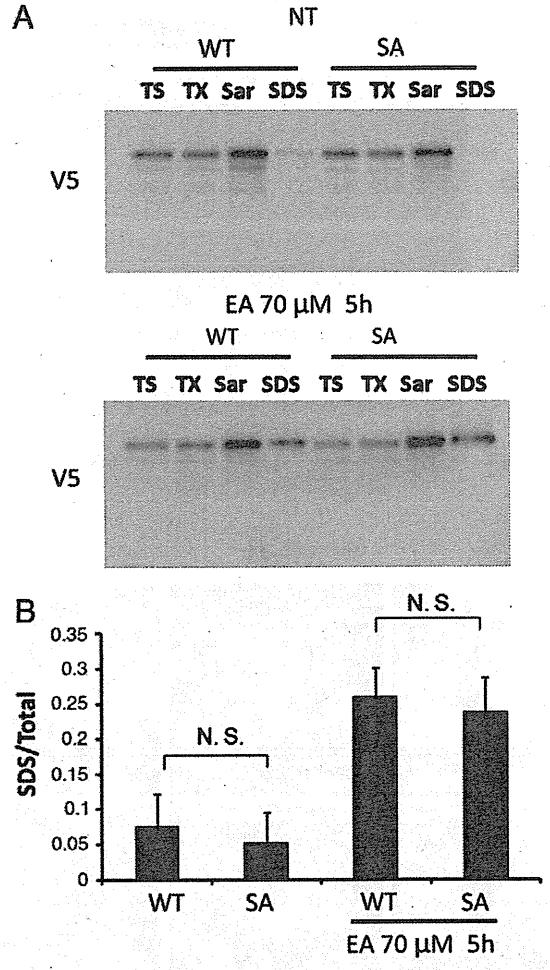

Fig. 7. The effect of C-terminal phosphorylation on TDP-43 solubility. (A) Sequential extraction of NSC34 cells expressing V5-WT- or V5-SA-TDP-43. (B) Densitometric quantitation of Sar-insoluble V5-TDP-43. Ratio of Sar-insoluble fraction from the whole fraction did not differ between WT- and SA-TDP-43 with or without 70 μM EA. Three independent experiments were performed. Error bars indicate SD.

In the present study, S403/404 and S409/410 of TDP-43 were phosphorylated together with insolubilization and cytoplasimic distribution of the protein. The hyperphosphorylation of disease marker proteins is a common feature of neurodegenerative disorders, and its relation to the pathogenesis has been intensively investigated: Tau in AD; huntingtin in HD; and alfa-synuclein in PD and DLB (Ballatore et al., 2007; Fujiwara et al., 2002; Gu et al., 2009). A number of studies have demonstrated that disease-specific phosphorylation of these marker proteins modulates aggregation and potentially influences disease pathogenesis (Azeredo da Silveira et al., 2009; Gu et al., 2009). In the present study, there was no difference between wild type and non-phosphorylable TDP-43 in the degree of insolubilization and cytoplasmic translocation under oxidative stress conditions, suggesting that C-terminal phosphorylation of TDP-43 is not mandatory for aggregation or abnormal intracellular distribution. In support with our findings, there is a study demonstrating that C-terminal phosphorylation of TDP-43 is not substantially required for the cytoplasmic aggregation (Brady et al., 2010). In addition, our results show that C-terminal tags interfere with the detection of TDP-43 phosphorylation, providing a cautionary note for cell-based and animal studies of TDP-43 with a C-terminal tag.

We further examined whether the pathological modifications of TDP-43 contribute to cell vulnerability to glutathione depletion. In the analysis of MTS assay, the viabilities of NSC34 cells were decreased by EA treatment. Although GFP-WT-TDP-43 was fully phosphorylated, insolubilized and distributed to cytoplasm in the cells treated with EA, there was no significant difference in the viability between the cells expressing GFP-mock and GFP-WT-TDP-43. In addition, the viability of NSC34 cells expressing GFP-SA-TDP-43 was not different from that of the cells expressing GFP-WT-TDP-43. These findings suggest that TDP-43 modification may not affect cell viability under oxidative stress induced by glutathione depletion.

In conclusion, we demonstrated that oxidative stress induced by glutathione depletion instigated TDP-43 modifications including C-terminal phosphorylation, insolubilization, C-terminal fragmentation and cytoplasmic distribution, and that these changes reproduce the pathological features of TDP-43 proteinopathies and other neurodegenerative diseases such as AD.

Supplementary materials related to this article can be found online at doi:10.1016/j.nbd.2011.12.002.

Funding

Funding: This work was supported by a Center-of-Excellence (COE) grant, a Grant-in-Aid for Scientific Research on Innovated Areas "Foundation of Synapse and Neurocircuit Pathology," and Grant-in-Aids from Ministry of Education, Culture, Sports, Science, and Technology of Japan; grants from the Ministry of Health, Labor and Welfare of Japan; and Core Research for Evolutional Science and Technology (CREST) of the Japan Science and Technology Agency (JST).

References

Abe, K., et al., 1995. Induction of nitrotyrosine-like immunoreactivity in the lower motor neuron of amyotrophic lateral sclerosis. Neurosci. Lett. 199, 152–154.

Abe, K., et al., 1997. Upregulation of protein-tyrosine nitration in the anterior horn cells of amyotrophic lateral sclerosis. Neurol. Res. 19, 124–128.
Amador-Ortiz, C., et al., 2007. TDP-43 immunoreactivity in hippocampal sclerosis and Alzheimer's disease. Ann. Neurol. 61, 435–445.
Arai, T., et al., 2006. TDP-43 is a component of ubiquitin-positive tau-negative inclusions in frontotemporal lobar degeneration and amyotrophic lateral sclerosis. Biochem. Biophys. Res. Commun. 351, 602–611.
Arai, T., et al., 2009. Phosphorylated TDP-43 in Alzheimer's disease and dementia with Lewy bodies. Acta Neuropathol. 117, 125–136.
Arai, T., et al., 2010. Phosphorylated and cleaved TDP-43 in ALS, FTLD and other neurodegenerative disorders and in cellular models of TDP-43 proteinopathy. Neuropathology 30, 170–181.
Ayala, Y.M., et al., 2005. Human, Drosophila, and C.elegans TDP43: nucleic acid binding properties and splicing regulatory function. J. Mol. Biol. 348, 575–588.
Ayala, Y.M., et al., 2008. TDP-43 regulates retinoblastoma protein phosphorylation through the repression of cyclin-dependent kinase 6 expression. Proc. Natl. Acad. Sci. U. S. A. 105, 3785–3789.
Azeredo da Silveira, S., et al., 2009. Phosphorylation does not prompt, nor prevent, the formation of alpha-synuclein toxic species in a rat model of Parkinson's disease. Hum. Mol. Genet. 18, 872–887.
Ballatore, C., et al., 2007. Tau-mediated neurodegeneration in Alzheimer's disease and related disorders. Nat. Rev. Neurosci. 8, 663–672.
Beal, M.F., et al., 1997. Increased 3-nitrotyrosine in both sporadic and familial amyotrophic lateral sclerosis. Ann. Neurol. 42, 644–654.
Brady, O.A., et al., 2010. Regulation of TDP-43 aggregation by phosphorylation and p62/SQSTM1. J. Neurochem. 116, 248–259.
Buratti, E., et al., 2005. TDP-43 binds heterogeneous nuclear ribonucleoprotein A/B through its C-terminal tail: an important region for the inhibition of cystic fibrosis transmembrane conductance regulator exon 9 splicing. J. Biol. Chem. 280, 37572–37584.
Buratti, E., et al., 2010. Nuclear factor TDP-43 can affect selected microRNA levels. FEBS J. 277, 2268–2281.
Butterfield, D.A., et al., 2007. Roles of amyloid beta-peptide-associated oxidative stress and brain protein modifications in the pathogenesis of Alzheimer's disease and mild cognitive impairment. Free Radic. Biol. Med. 43, 658–677.
Caragounis, A., et al., 2010. Zinc induces depletion and aggregation of endogenous TDP-43. Free Radic. Biol. Med. 48, 1152–1161.
Colombrita, C., et al., 2009. TDP-43 is recruited to stress granules in conditions of oxidative insult. J. Neurochem. 111, 1051–1061.
Dormann, D., et al., 2009. Proteolytic processing of TAR DNA binding protein-43 by caspases produces C-terminal fragments with disease defining properties independent of progranulin. J. Neurochem. 110, 1082–1094.
Ferrante, R.J., et al., 1997. Evidence of increased oxidative damage in both sporadic and familial amyotrophic lateral sclerosis. J. Neurochem. 69, 2064–2074.
Frederickson, C.J., et al., 2005. The neurobiology of zinc in health and disease. Nat. Rev. Neurosci. 6, 449–462.
Fujiwara, H., et al., 2002. alpha-Synuclein is phosphorylated in synucleinopathy lesions. Nat. Cell Biol. 4, 160–164.
Geser, F., et al., 2008. Pathological TDP-43 in parkinsonism-dementia complex and amyotrophic lateral sclerosis of Guam. Acta Neuropathol. 115, 133–145.
Gu, X., et al., 2009. Serines 13 and 16 are critical determinants of full-length human mutant huntingtin induced disease pathogenesis in HD mice. Neuron 64, 828–840.
Hasegawa, M., et al., 2007. TDP-43 is deposited in the Guam parkinsonism-dementia complex brains. Brain 130, 1386–1394.
Hasegawa, M., et al., 2008. Phosphorylated TDP-43 in frontotemporal lobar degeneration and amyotrophic lateral sclerosis. Ann. Neurol. 64, 60–70.
Igaz, L.M., et al., 2009. Expression of TDP-43 C-terminal Fragments in Vitro Recapitulates Pathological Features of TDP-43 Proteinopathies. J. Biol. Chem. 284, 8516–8524.
Iguchi, Y., et al., 2009. TDP-43 depletion induces neuronal cell damage through dysregulation of Rho family GTPases. J. Biol. Chem. 284, 22059–22066.
Keelan, J., et al., 2001. Quantitative imaging of glutathione in hippocampal neurons and glia in culture using monochlorobimane. J. Neurosci. Res. 66, 873–884.
Liu-Yesucevitz, L., et al., 2010. Tar DNA binding protein-43 (TDP-43) associates with stress granules: analysis of cultured cells and pathological brain tissue. PLoS One 5, e13250.
Lovell, M.A., Markesbery, W.R., 2007. Oxidative DNA damage in mild cognitive impairment and late-stage Alzheimer's disease. Nucleic Acids Res. 35, 7497–7504.
McDonald, K.K., et al., 2011. TAR DNA-binding protein 43 (TDP-43) regulates stress granule dynamics via differential regulation of G3BP and TIA-1. Hum. Mol. Genet. 20, 1400–1410.
Migliore, L., 2005. Searching for the role and the most suitable biomarkers of oxidative stress in Alzheimer's disease and in other neurodegenerative diseases. Neurobiol. Aging 26, 587–595.
Moisse, K., et al., 2009. Divergent patterns of cytosolic TDP-43 and neuronal progranulin expression following axotomy: implications for TDP-43 in the physiological response to neuronal injury. Brain Res. 1249, 202–211.
Neumann, M., et al., 2006. Ubiquitinated TDP-43 in frontotemporal lobar degeneration and amyotrophic lateral sclerosis. Science 314, 130–133.
Nishimoto, Y., et al., 2010. Characterization of alternative isoforms and inclusion body of the TAR DNA-binding protein-43. J. Biol. Chem. 285, 608–619.
Nonaka, T., et al., 2009a. Phosphorylated and ubiquitinated TDP-43 pathological inclusions in ALS and FTLD-U are recapitulated in SH-SY5Y cells. FEBS Lett. 583, 394–400.
Nonaka, T., et al., 2009b. Truncation and pathogenic mutations facilitate the formation of intracellular aggregates of TDP-43. Hum. Mol. Genet. 18, 3353–3364.
Nunomura, A., et al., 2002. Neuronal RNA oxidation is a prominent feature of dementia with Lewy bodies. Neuroreport 13, 2035–2039.
Polymenidou, M., et al., 2011. Long pre-mRNA depletion and RNA missplicing contribute to neuronal vulnerability from loss of TDP-43. Nat. Neurosci. 14, 459–468.
Rizzardini, M., et al., 2003. Mitochondrial dysfunction and death in motor neurons exposed to the glutathione-depleting agent ethacrynic acid. J. Neurol. Sci. 207, 51–58.
Sato, T., et al., 2009. Axonal ligation induces transient redistribution of TDP-43 in brainstem motor neurons. Neuroscience 164, 1565–1578.
Sephton, C.F., et al., 2011. Identification of neuronal RNA targets of TDP-43-containing ribonucleoprotein complexes. J. Biol. Chem. 286, 1204–1215.
Shaw, I.C., et al., 1995. Studies on cellular free radical protection mechanisms in the anterior horn from patients with amyotrophic lateral sclerosis. Neurodegeneration 4, 391–396.
Strong, M.J., et al., 2007. TDP43 is a human low molecular weight neurofilament (hNFL) mRNA-binding protein. Mol. Cell. Neurosci. 35, 320–327.
Tollervey, J.R., et al., 2011. Characterizing the RNA targets and position-dependent splicing regulation by TDP-43. Nat. Neurosci. 14, 452–458.
Wang, I.F., et al., 2002. Higher order arrangement of the eukaryotic nuclear bodies. Proc. Natl. Acad. Sci. U. S. A. 99, 13583–13588.
Wang, H.Y., et al., 2004. Structural diversity and functional implications of the eukaryotic TDP gene family. Genomics 83, 130–139.
Winton, M.J., et al., 2008. Disturbance of nuclear and cytoplasmic TAR DNA-binding protein (TDP-43) induces disease-like redistribution, sequestration, and aggregate formation. J. Biol. Chem. 283, 13302–13309.
Zhang, Y.J., et al., 2007. Progranulin mediates caspase-dependent cleavage of TAR DNA binding protein-43. J. Neurosci. 27, 10530–10534.

The FASEB Journal • Research Communication

Phosphorylated α-synuclein can be detected in blood plasma and is potentially a useful biomarker for Parkinson's disease

Penelope G. Foulds,* J. Douglas Mitchell,‡ Angela Parker,‡ Roisin Turner,‡ Gerwyn Green,† Peter Diggle,† Masato Hasegawa,§ Mark Taylor,* David Mann,‖ and David Allsop*,[1]

*Division of Biomedical and Life Sciences and †Division of Health Research, School of Health and Medicine, University of Lancaster, Lancaster, UK; ‡Royal Preston Hospital, Preston, UK; §Department of Molecular Neurobiology, Tokyo Institute of Psychiatry, Tokyo, Japan; and ‖Neurodegeneration and Mental Health Research Group, School of Community-Based Medicine, University of Manchester, Hope Hospital, Salford, UK

ABSTRACT **Parkinson's disease (PD) is characterized by the presence of Lewy bodies containing phosphorylated and aggregated α-synuclein (α-syn). α-Syn is present in human body fluids, including blood plasma, and is a potential biomarker for PD. Immunoassays for total and oligomeric forms of both normal and phosphorylated (at Ser-129) α-syn have been used to assay plasma samples from a longitudinal cohort of 32 patients with PD (sampled at mo 0, 1, 2, 3), as well as single plasma samples from a group of 30 healthy control participants. The levels of α-syn in plasma varied greatly between individuals, but were remarkably consistent over time within the same individual with PD. The mean level of phospho-α-syn was found to be higher (P=0.053) in the PD samples than the controls, whereas this was not the case for total α-syn (P=0.244), oligo-α-syn (P=0.221), or oligo-phospho-α-syn (P=0.181). Immunoblots of plasma revealed bands (at 21, 24, and 50–60 kDa) corresponding to phosphorylated α-syn. Thus, phosphorylated α-syn can be detected in blood plasma and shows more promise as a diagnostic marker than the nonphosphorylated protein. Longitudinal studies undertaken over a more extended time period will be required to determine whether α-syn can act as a marker of disease progression.—Foulds, P. G., Mitchell, J. D., Parker, A., Turner, R., Green, G., Diggle, P., Hasegawa, M., Taylor, M., Mann, D., Allsop, D. Phosphorylated α-synuclein can be detected in blood plasma and is potentially a useful biomarker for Parkinson's disease. *FASEB J.* 25, 4127–4137 (2011). www.fasebj.org**

Key Words: Lewy body · oligomer · immunoassay · immunoblot

PARKINSON'S DISEASE (PD) is the second most common neurodegenerative disorder after Alzheimer's disease (AD) and is characterized clinically by the 3 cardinal motor symptoms of resting tremor, rigidity, and bradykinesia. Patients often exhibit further symptoms, including postural imbalance, gait disturbance, and a mask-like facial expression. In the advanced stages of PD, nonmotor symptoms can also appear, including anxiety, depression, dementia, and psychosis. The defining neuropathological features of idiopathic PD are the loss of dopaminergic neurons from the substantia nigra (SN) and the presence of Lewy bodies (LBs) and Lewy neurites (LNs) in surviving neurons of this and other brain regions (1). Similar lesions are present within the cerebral cortex in the related disorder of dementia with Lewy bodies (DLB; ref. 2). LBs and LNs contain a misfolded, fibrillar, and phosphorylated form of the protein α-synuclein (α-syn; refs. 1, 3). Pathological changes involving α-syn, chiefly in glial cells, also occur in multiple system atrophy (MSA), and, therefore, PD, DLB, and MSA are often collectively referred to as "α-syncleinopathies" (2). Duplication (4, 5), triplication (6), and mutation (7–9) of the gene encoding α-syn (*SNCA*) are all causes of hereditary forms of either PD or DLB. α-Syn oligomers are believed to be toxic to cells, as are oligomers derived from the various proteins associated with several other protein-misfolding neurodegenerative disorders, such as AD or the prion disorders (10, 11). Overexpression of wild-type or mutant α-syn in animal models can produce a phenotype resembling PD, including SN degeneration, movement problems and responsiveness to L-dopa therapy (12–15). Together, these observations suggest that α-syn plays a pivotal role in the development of the α-synucleinopathies (16).

PD is one of several neurological movement disor-

[1] Correspondence: Division of Biomedical and Life Sciences, School of Health and Medicine, University of Lancaster, Lancaster, LA1 4AY, UK. E-mail: d.allsop@lancaster.ac.uk

doi: 10.1096/fj.10-179192

This article includes supplemental data. Please visit *http://www.fasebj.org* to obtain this information.

0892-6638/11/0025-4127 © FASEB